Ecological Modelling 250 (2013) 81–100

Contents lists available at SciVerse ScienceDirect

Ecological Modelling

journal homepage: www.elsevier.com/locate/ecolmodel

# A hierarchical patch mosaic ecosystem model for urban landscapes: Model development and evaluation

Chi Zhang[a,b,*], Jianguo Wu[b,c,d], Nancy B. Grimm[b,d], Melissa McHale[b,e], Alexander Buyantuyev[c,d]

[a] State Key Laboratory of Desert and Oasis Ecology, Xinjiang Institute of Ecology and Geography, Chinese Academy of Sciences, Urumqi, Xinjiang, China
[b] Global Institute of Sustainability, Arizona State University, AZ, United States
[c] Sino-US Center for Conservation, Energy and Sustainability Science (SUCCESS), Inner Mongolia University, Hohhot 010021, China
[d] School of Life Sciences, Arizona State University, Tempe, AZ, United States
[e] College of Natural Resources, North Carolina State University, NC, United States

ARTICLE INFO

*Article history:*
Received 20 May 2012
Received in revised form
23 September 2012
Accepted 25 September 2012

*Keywords:*
Process-based model
Urban ecosystem
Carbon cycle
Hierarchical patch dynamics paradigm
Phoenix metropolitan area
LTER

ABSTRACT

Urbanization effects on ecosystem functions are both important and complex, characterized by scale multiplicity, spatial heterogeneity, and intensive human disturbances. Integrating the hierarchical structure of urban landscape pattern with ecosystem processes through simulation modeling can facilitate our understanding of human–environment interactions in urban environment. Current ecosystem models often focus on plant physiological and biogeochemical processes in homogeneous land covers, incapable of addressing the structural complexity in urban landscapes with multiple anthropogenic drivers across a range of spatial scales. Here we present the Hierarchical Patch Mosaic-Urban Ecosystem Model (HPM-UEM), a multi-scaled model that explicitly treats spatial pattern and hierarchical structure of urban landscape by incorporating both top-down controls and bottom-up mechanisms in urban environment. By addressing six hierarchical levels from individual plant to the urbanized region, HPM-UEM provides a "hierarchical ladder" to scale up local ecosystem functions across the nested urban land hierarchies (i.e., land cover, land use, landscape, and the urbanized region), and facilitate linking ecosystem processes and socioeconomic drivers. By organizing human influences in a spatially nested hierarchical patch mosaic structure, HPM-UEM models the complex spatiotemporal pattern of multiple environmental constraints on urban ecosystem functions. The model was evaluated based on extensive datasets developed by the Long-Term Ecological Research (LTER) network, especially the Central Arizona-Phoenix (CAP) LTER. Model testing results showed that HPM-UEM predicted both C fluxes and spatial pattern of C stocks with reasonable accuracy. HPM-UEM enabled us to assess spatial patterns and multiple-scaled dynamics of C cycle of the urban landscape, revealing the distinct productivities and C densities of different urban land types across different spatial scales. Sensitivity analyses indicated that future environmental changes and landscape modifications could have strong and complex effects on urban ecosystem functions. By matching ecological processes, anthropogenic environmental controls, and land and socioeconomic dynamics based on hierarchical levels, HPM-UEM could be coupled to multiple-scaled urban land-use models, climate models, and socioeconomic models to gain a comprehensive understanding of urban biogeochemical cycles.



## 1. Introduction

Humans have transformed about one-third to one-half of the earth's land surface, substantially altering the global biogeochemical cycle (Vitousek et al., 1997). Of different forms of land transformation, urbanization is arguably the most profound and complex, and has dominated land-use changes since the mid-20th century. In the United States, for example, urban and developed areas increased from 3.9% in 1982 to 5.2% in 1997 and were projected to reach 9.2% in 2025 (Alig et al., 2004). Globally, urbanized land is expected to increase by about one million km$^2$ over the next 25 years (McDonald, 2008). Numerous studies have indicated that urbanization has profound impacts on the productivity and C balance of terrestrial ecosystems from regional to continental scales (Imhoff et al., 2004; Pataki et al., 2006; Schaldach and Alcamo, 2007; Churkina, 2008; Svirejeva-Hopkins et al., 2004; Buyantuyev and Wu, 2009). Zhang et al. (2012) estimated that urban and developed land accounts for about 6.7–7.6% of total ecosystem C storage within the southern United States (US), larger than the pool size of shrubland.

Using urban vegetation to offset fossil C emissions has been proposed as a strategy to mitigate some of the negative impacts

* Corresponding author. Tel.: +86 18690321105; fax: +86 9917885320.
*E-mail address:* zhchbob@gmail.com (C. Zhang).

0304-3800/$ – see front matter © 2012 Elsevier B.V. All rights reserved.
http://dx.doi.org/10.1016/j.ecolmodel.2012.09.020

of urbanization (McPherson 1998; Nowak, 2006; Young, 2010; Zhao et al., 2010). Such projects require multi-disciplinary cooperation between ecologists, urban geologists, social scientists, and policy makers. However, urban ecologists frequently find communication between disciplines difficult due to the differences in terminologies. For example, when ecologists mention land types, they usually mean lands of homogeneous vegetation such as grassland or broadleaf forests. In contrast, when land-use modelers or economists mention land types, they often refer to the usage of the land in relation to certain socioeconomic functions (i.e., land-use), such as residential or commercial areas that consist of both impervious surfaces and green-space. For urban management, the C storage of an urban park is more meaningful to policy makers than the C density of a turfgrass ecosystem. The dilemma reflects the fact that ecologists work on a different research scale from the other groups. While ecologists focus on the ecophysiology of plants and ecological functions of local ecosystems (or land-covers) that are usually small pieces of urban land fragments with relatively homogeneous land surface, social scientists and policy makers are more interested in the socioeconomic functions of the land-uses and landscapes (e.g., towns or agricultural lands) that usually have a larger spatial extent and heterogeneous surface structure. It is, therefore, important to develop a scaling tool to extrapolate the ecosystem functions (e.g., the net primary productivity, or NPP) on the land-cover level to land-use or even landscape scales. Such scaling is possible because urban land use is composed of multiple land covers (e.g., a residential area consists of impervious surfaces, lawns, and yard trees), forming a nested structure.

It has been suggested that the urban land complexity takes the form of hierarchy, whereby a complex system consists of interrelated subsystems that are in turn composed of their own subsystems, and so on, until the level of elementary or "primitive" components is reached (descriptions of the Hierarchy Theory are found in O'Neill et al. (1986) and Wu (1999)). In this two-leveled hierarchy, land cover is the elementary level. According to Wu and David (2002), there are two other hierarchical levels above the land-use scale: the landscape level and region level. Landscape is composed of multiple land-use patches in which spatial patterns emerge, and characterized by the dominant land-use types (e.g., urban, rural, agricultural, and natural landscapes). Region is a mixture of landscapes, and characterized by its socioeconomic background (e.g., a North American metropolitan region vs. an East Asian metropolitan region), as well as its biogeophysical background, such as climate, geomorphology, hydrology, soils, and vegetation at the regional scale (e.g., a desert metropolitan region vs. an agricultural grassland region). The land use → landscape → region hierarchy (→ indicates the scaling up direction) of urban land structure reflects the hierarchical structure of human society (i.e., neighborhood/district → town/city → metropolitan region/economic zone), and has already been incorporated in hierarchical socioeconomic and land-use models (Veldkamp and Fresco, 1996; Moreira et al., 2009). Adding the land-cover/local ecosystem level to the urban land hierarchy could help us to link ecological processes to the complex urban land structure (including patterns of the environmental constraints) and the underlying socioeconomic dynamics (see the Appendix Fig. A1). By modeling the bottom-up mechanisms and top-down constraints in the urban hierarchy (O'Neill et al., 1986), ecosystem functions (e.g., NPP) can be scaled up from the land-cover level all the way to regional level along the "hierarchical scaling ladder" (Wu, 1999; Jenerette, 2004), assessing ecosystem services by various land types to support urban ecosystem management.

The hierarchical urban ecosystem model is also required for addressing the multiple anthropogenic and environmental drivers that work on different scales. Urban ecosystem functions have been dramatically affected from local to global scales by human management (Martin and Stabler, 2004) and anthropogenic environmental changes in climate (Arnfield, 2003) and atmosphere (Lohse et al., 2008). The impacts of global climate change (Chen et al., 2012), urban-induced environmental changes (Shen et al., 2008; Trusilova and Churkina, 2008), and urban land-use management (Milesi et al., 2005) have been individually investigated in separate modeling studies, however, no study has considered all of these three types of environmental controls that act on different scales. On the regional scale, climate and atmospheric changes caused by anthropogenic greenhouse gas emissions determine the background environmental conditions in urban ecosystems. On the landscape level, urban-induced environmental changes such as urban heat islands (UHI) and $CO_2$ dome effects (Idso, 2001; Arnfield, 2003) could modify the environmental variables. On the land-use scale, intensive management (e.g., irrigation and landscaping) and introduction of exotic species could further alter the microclimate, and directly modify the structure and biogeochemical cycles of local ecosystems (Pouyat and Carreiro, 2003; Jenerette et al., 2007). Correctly modeling the hierarchical structure of anthropogenic controls is not only important for revealing the complex spatial patterns of human disturbances and their effects on ecosystem functions (Grimm et al., 2008a), but also helpful for linking anthropogenic controls to socioeconomic processes on their corresponding scales (see the Appendix Fig. A1).

In addition to the urban land structure, the hierarchy of the ecological organization (i.e., individual plant → population → local ecosystem) was also inadequately addressed in current urban models (e.g., Nowak and Crane, 2000). The individual plant and population levels, together with the related ecological processes such as population dynamics, were generally overlooked. Without considering population dynamics, vegetation competition for energy and nutrients cannot be modeled. Former studies had to assume that a single vegetation type occupied each land cover. In contrast, George et al. (2009) and Ziska et al.'s (2004) studies in Baltimore, MD, indicated that long-term, urban-induced environmental changes could trigger community succession that altered ecosystem functions such as NPP, highlighting the importance of considering population dynamics in urban areas. Without information of plant structure, urban vegetation management, such as tree pruning, cannot be modeled, and important ecological services such as the effect of tree shade on home energy usage (Nowak and Crane, 2000) cannot be estimated. Furthermore, information about crown size and canopy coverage is important for modeling energy partition in ecosystem, especially for open canopies commonly found in urban forests. Without such information, most models used the two-stream energy partition scheme that assumes a homogeneous canopy with 100% land coverage (Sellers, 1985), which could result in up to 40% overestimation of the leaf-absorbed solar radiation when applied to open canopies (Yang et al., 2001). Therefore, the ecosystem hierarchical levels, such as the plant population and the individual plant levels should be explicitly addressed in urban ecosystem modeling.

In general, urbanization alters biotic and abiotic ecosystem properties from local to continental scales (Grimm et al., 2008a), and urban ecosystems are affected by various anthropogenic and environmental factors across multiple scales (Grimm et al., 2008b). A hierarchical ecosystem model can help deal with urban ecosystem complexities, and conduct cross-scaled studies to gain a complete picture of urban biogeochemical cycles (Grimm et al., 2008a). Based on the conceptual model of Hierarchical Patch Dynamics (Wu, 1999; Wu and David, 2002; Wu et al., 2003), this study developed a Hierarchical Patch Mosaic–Urban Ecosystem Model (HPM-UEM) that includes six nested hierarchical levels: individual plant → population → land-cover (or local ecosystem) → land-use → landscape → region. The biophysical and ecophysiological processes at and below the local ecosystem scale

were modeled based on knowledge from natural ecosystems, with C, water, and N cycles coupled (Niemelä, 1999; Groffman et al., 2006). At higher levels, factors associated with land management, landscape patterns, and multiple environmental changes (e.g., climatic conditions, $CO_2$, and N deposition) were explicitly incorporated into the spatially nested urban land hierarchy. To address the spatial heterogeneity in the landscape and environments, urban lands were treated as spatially nested patch mosaics in the HPM-UEM. By modeling the top-down constraints and bottom-up mechanisms in urban hierarchy, HPM-UEM aims to: (1) provide a "hierarchical scaling ladder" to extrapolate the local ecosystem functions from the land-cover to the land-use, landscape, and regional levels, and facilitate linking ecosystem processes to the socioeconomic factors that control the urban land structure; (2) model the nested structure of human disturbances, assessing how multiple anthropogenic controls from different scales modify the environmental factors that constrain ecosystem functions; and (3) address two important yet frequently overlooked ecosystem hierarchical levels - the population and individual plant levels, and explicitly model the related plant/population structure and processes. To evaluate the performance of the model, we applied it in a comprehensive analysis of ecosystem productivity and C storage in the Phoenix metropolitan region, Arizona, USA. It should be noted that HPM-UEM focuses primarily on ecosystems in the urban region; material and energy fluxes related to human and industrial consumption are beyond the scope of this study. Possibilities of coupling HPM-UEM to socioeconomic, climate, and land-use change models for a more dynamic and comprehensive urban ecosystem study are discussed.

## 2. Description of the model structure

According to the hierarchy theory, complex systems have both a vertical structure that is composed of levels, and a horizontal structure that consists of holons (Simon, 1962). Each hierarchical level is characterized by a group of processes that have similar process rates (e.g., behavioral frequencies or response times). The upper level exerts constraints on the lower level, whereas the lower provides mechanistic explanation for higher levels. Considering the important influences of landscape configuration (i.e., relative location and size of different land-uses) on socioeconomic and land-use dynamics in human-dominated ecosystems like urban areas, Wu and David (2002) proposed to treat the land patch, a spatially continuous land unit that provides basic socioeconomic functions, as the "holon" in an urban landscape hierarchy. Following Wu and David (2002), this model treats urban land as spatially nested hierarchical patch mosaics, which organizes a large number of local land patches into progressively fewer, larger patches with similar functional properties under the same anthropogenic environmental controls, together forming a spatially nested hierarchy. A land patch in HPM-UEM was characterized by a unique identification number (ID), the hierarchical level, location, size, shape, and content of its structure (the IDs of all componential patches or holons). To address the location, size, and shape of land patches, as well as the spatial heterogeneity in the background biogeophysical and environmental constraints (i.e., geomorphology, soils, climate, and atmosphere), a study region was segmented into a reference matrix, whereby each grid (or pixel) had a unique grid ID, fixed size and shape, and a pre-known location with latitude/longitude coordinates. A grid was assumed to have a homogeneous background biogeophysical and environmental constraints. Landscape configuration was determined by overlaying urban land maps on the reference matrix. A land patch can occupy one or more reference grids, while a grid refers to multiple nested land patches, each belonging to a different hierarchical level. Patch dynamics can be modeled by updating the grid IDs in a changed patch. When the land-cover type of a grid is converted to a different type, the original local ecosystem loses all its vegetation C into the litter and product pools (e.g., the woody products from a harvested forest), and its soil biogeochemical pools could be disturbed. Detailed descriptions of how the effects of these disturbances were modeled in HPM-UEM with a parametric approach are provided in the Section 2.2. Because parameters that define the ecosystem disturbances during land-cover changes were unavailable, the patch dynamics were not simulated in the Phoenix metropolitan case study (see below).

The composition, location, and human disturbances (e.g., air pollution or land management) of an land patch could have significant impacts on ecosystem functions by influencing the vegetation structure such as the green-space coverage, environmental controls like local climate and $CO_2$ concentration (Wentz et al., 2002), and biogeochemical cycles like water input from irrigation (Milesi et al., 2005). Therefore, the HPM-UEM emphasizes the top-down anthropogenic environmental controls from the landscape and land-use levels on local ecosystem functions, which were then aggregated to assess ecosystem functions at land-use, landscape, and regional levels. By treating urban landscapes as spatially nested hierarchical patch mosaics and addressing the anthropogenic environmental changes in each patch, HPM-UEM reveals the complex spatial pattern of urban environments (climate, $CO_2$ concentration, and N deposition), and models how human disturbances and management at different scales can affect ecosystem functions by modifying the environmental constraints.

HPM-UEM explicitly considers the hierarchical structure of the urban landscape, land management practices, and interactions among biogeochemical processes on multiple scales ranging from the individual plant to metropolitan regions (Fig. 1). At each scale in the hierarchical structure, the dominant system processes together with their environmental drivers and constraints were modeled. Detailed descriptions of each hierarchical level and their related ecosystem processes and environmental controls can be found in the following sections, and are listed in Table 1. In model application, HPM-UEM first determines the background biogeophysical and environmental conditions in each reference grid. Then, in a top-down sequence, the spatial properties and biogeophysical/environmental backgrounds of land patches at each hierarchical level were initialized by overlaying land maps (of different hierarchical levels) against the reference matrix. Next, in a top-down sequence, the environmental conditions of each land patch are modified by the anthropogenic controls including regional climate changes, urban-induced environmental changes, and the microclimate changes induced by land-use management, like the cooling effect of irrigation. Finally, constrained by local environments and land-use management regimes, ecological processes (e.g., seedling establishment, growth, mortality, and organic matter decomposition) in each land-cover grid were modeled. The ecosystem structure and functions at each hierarchical level were estimated with simple extrapolation, e.g., the C storage of a residential area was calculated by summing the C storage of its componential patches such as impervious surfaces, lawns, yard trees, etc. (Wu, 1999).

### 2.1. Description of the land-cover, land-use, landscape, and regional hierarchical levels

The land-cover, also addressed as a local ecosystem, is defined as relatively homogeneous, biophysical cover of the earth's surface (e.g., urban forest, impervious surface, or cotton field). A land-cover patch in the HPM-UEM is a vegetation-soil complex composed of multiple plant populations, as well as the litter and soil organic pools. To improve simulation efficiency, plant species were grouped into several plant functional types (PFT; e.g., C3 grass, shrubs,

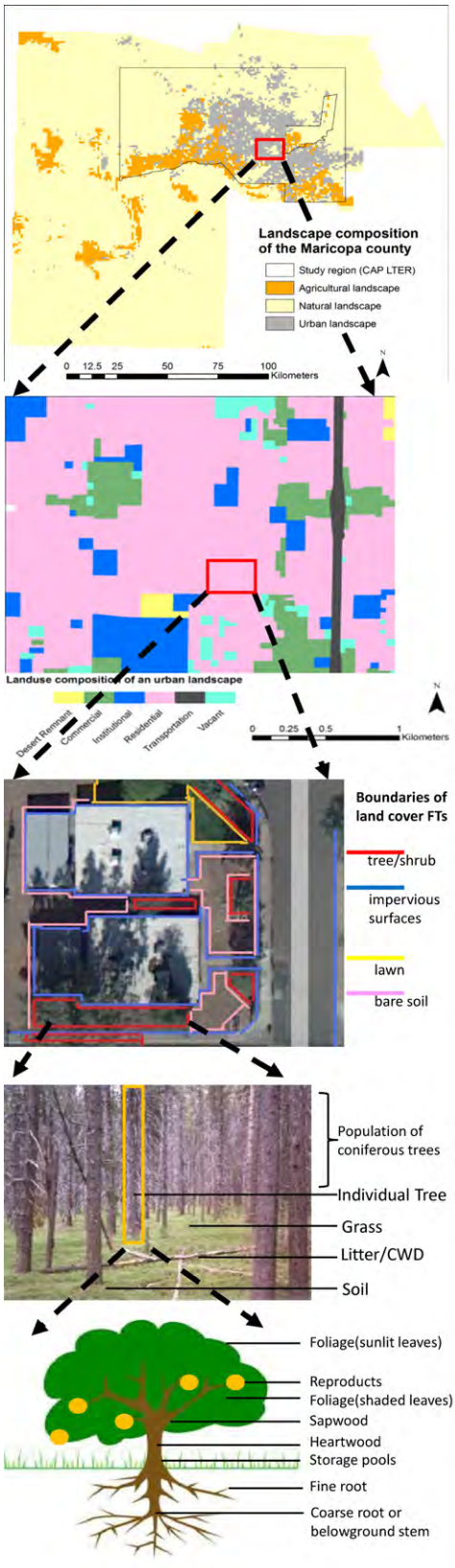


| Hierarchical level | Components and attributes (examples) | Processes (examples) |
|---|---|---|
| Region | Spatial arrangement of landscape patches (urban, agriculture, natural land), & the background biophysical constrains (soil type, elevation, climate); characterized by the dominant biome & the regional land-use pattern (e.g., an urbanized desert region vs. an agricultural grassland region) | Global changes (climate, $CO_2$, regional air pollution, land-use changes ). The regional land-use pattern is linked to socioeconomic processes *. |
| Landscape | Spatial pattern of land-use patches (industrial/commercial, residential, transportation, riparian zone) | Local environmental changes * (urbanization induced environmental changes in climate and atmosphere) |
| Land-use | Composition of land-cover types and their management regimes (impervious surface, forest, lawn, bare soil) | Managements and their environmental effects * (fertilization, pruning, harvest, irrigation and its cooling effect) |
| Land-cover (or local ecosystem) | Populations of plant functional types (broadleaf tree, C4/C3 grass, shrub), coarse woody debris (CWD), litter pools, soil organic matter pools, etc. | Energy partition, water balance, soil processes, competition & succession, etc. |
| Population of plant functional type (PFT) | Number of individual plants | Regeneration & mortality, aggregated ecological functions (NPP, carbon storage) of the PFT, etc. |
| Average individual plant | Plant organs (leaf, root, stem, reproducts, carbon & nitrogen storage pools) | Photosynthesis, water & nitrogen uptake, organ turnover, growth and allocation. |

* With a client/server software engineering structure, interfaces have been developed to link the HPM-UEM to socioeconomic and regional climate models, although the HPM-UEM itself does not model any socioeconomic or climate processes.

**Fig. 1.** Illustration of the six hierarchically nested ecosystem levels modeled by the HPM-UEM.

**Table 1**
Hierarchical structure, relevant spatiotemporal scales, dominant processes, models and assumptions, constraints, and outputs for ecosystem functional types at six hierarchical levels (major rows), as modeled by the HPM-UEM.

| Hierarchical level | Functional type | Structure (components) | Scale (spatial; temporal) | Processes | Major submodels and assumptions | Constrains and drivers | Outputs (examples) |
|---|---|---|---|---|---|---|---|
| Individual plant | Tree, grass, shrub | Organs: leaf, root, reproductive and storage organ, stem | 1–10 m; day to year | Productivity, transpiration, N uptake, growth and allocation of biomass to organs | Photosynthesis (Farquhar model). Energy balance (Penman–Monteith equation). Allocation (pipe model and allometric equations). Assumption: stoichiometric C:N ratio of organ and litter | Physiological parameters of the PFT, resource (light, N, water) availability, biophysical constrains (temperature, $CO_2$, etc.) | Biomass, transpiration rate, productivity and litter-fall rate of plant; crown size, height, DBH of tree |
| Population of plant functional types (PFT) | Population of tree (coniferous, broadleaf), grass (C3, C4), crop, shrub | Number of individual plants per square meter | Neighbor-hood; day to year | Regeneration, mortality | Average plant individual approach (Sitch et al., 2003). Management and disturbance regimes are same in a population | Bioclimatic constraints (Haxeltine and Prentice, 1996), resource availability | C, N, water fluxes, biomass on the population level |
| Land-cover (or local ecosystem) | natural ecosystem, monoculture, cropland, impervious surface | PFTs, soil (water, SIN, DON, SOM, litter, CWD), ecosystem products | Neighbor-hood; day to year | Resource competition and succession; canopy energy partition; soil processes: decomposition, N mineralization, trace-gas emission, water runoff | Assumption: Homogeneous biotic and abiotic resources shared by all plants in the same community (i.e., land cover unit) | Microclimate (precipitation, daily temperature, humidity), $CO_2$, N deposition, latitude, slope, aspect, soil texture | C, N, water fluxes; plant community, soil, product pools; FPC, coverage of PFTs |
| Land-use (LU) | Residential, transportation, commercial, agricultural, riparian, undisturbed land | LC types and management regimes | Neighbor-hood or larger; year to decade | Management on LCs (e.g., lawn irrigation, fertilization, clipping, tree pruning, cropland fertilization) | Assumption: a LU type has relatively stable structure (i.e., composition and coverage of the componential LCs) and management regime | Social-economic backgrounds and environmental policy determine the structure and management regimes of a LU[a] | Biogeochemical processes at the land-use scale and their responses to management |
| Landscape | Natural ecosystem, plantation, agriculture, urban | Spatial distribution of multiple LU patches | Usually >1 ha; decade | Changes in local climate and atmosphere (e.g., UHI, $CO_2$ dome, elevated N deposition) | Assumption: ecosystem function is affected by its spatial pattern. Spatial patterns of LU patches and environmental drivers can be derived from remote sensing, observation (spatial interpolation), empirical or process-based land-use change models[a] | Land planning and environmental policy[a] spatial pattern of environmental factors | Spatial patterns of biogeochemical fluxes and pool at the landscape level |
| Region | For example, Arizona, Southwest, USA, or global scale | Landscape patches | State to global level; decade to century | Land-use changes: urbanization, cropland conversion etc., and regional climate changes | Historical land-use census data or future land use projected by patch-dynamic models | Global changes in response to social-economic development and environmental policy | Biogeochemical cycles at regional to global levels |

[a] HPM-UEM prepares interfaces to social-economic models (see Appendix Fig. A1). In the Phoenix case study, however, social-economic models were not linked to HPD-UEM. Instead, parametric approaches were used to address the patterns of landscape and land managements in Phoenix, AZ.

or broadleaf trees) according to their ecophysiological characteristics (Box, 1981). Important biogeochemical processes such as solar energy partition, water evaporation and transpiration, and soil organic matter decomposition were modeled at this hierarchical level. Because the HPM-UEM explicitly models population dynamic (i.e., seedling establishment, growth, and mortality), multiple PFT populations can coexist in a land-cover patch, competing for light, nutrients, and water resources. In contrast, popular models like CENTURY (Parton et al., 1988) and BIOME-BGC (Running and Coughlan, 1988) cannot address population dynamics, assuming that each land cover has only one vegetation type. Such an assumption may improve computational efficiency when a high-resolution vegetation map is available for the study region, but cannot predict vegetation dynamic/succession in response to the anthropogenic environmental changes in urban areas (George et al., 2009). HPM-UEM models population dynamics even for monocultural ecosystems (e.g., forest plantation), to simulate the effects of urban forest management, such as selective harvest, on canopy structure and energy partition (Yang et al., 2001).

Land use (e.g., road network, park) is a patch mosaic of land-covers that are allocated, modified, and managed to provide certain socioeconomic functions such as transportation or recreation. In another words, a land-use type represents how the land is used for certain social and economic functions (Wang and Zhang, 2001). Since the structure of a land-use type is constrained by its social and economic functions, HPM-UEM assumes that the land-cover composition of a land-use type is relatively stable and influenced by cultural, economic, and biogeophysical backgrounds at the region level (see below) (Martin et al., 2003; Svirejeva-Hopkins et al., 2004). Li et al. (2011) found that the composition and spatial pattern of land covers were stable within the same land use, but differed among different land uses in Beijing, China. Parameters that define the structure (i.e., land-cover composition) of land-use types can be derived from field observations (as in the Phoenix metropolitan case study described below) or by overlaying the land-use map on a land-cover map with relatively high spatial resolution.

In additional to its socioeconomic properties, land uses in HPM-UEM were characterized by their management regimes (e.g., xeric residential area vs. mesic residential area), which could have significant impacts on ecosystem functions (Martin and Stabler, 2004). Many studies mixed land-use types with land-cover types. Treating the land-cover and the land-use hierarchical levels separately, however, is the key to linking ecosystem functions to socioeconomic processes as mentioned in the "Introduction section" of this study. HPM-UEM emphasizes that while ecosystem processes dominate the hierarchical levels at and below the land-cover scale, socioeconomic processes dominate the hierarchical levels at and above the land use scale. The land-use and anthropogenic environmental changes (e.g., air pollution) driven by socioeconomic dynamics at the land-use or landscape scales could have strong impacts on local ecosystem processes.

A landscape (e.g., urban, agricultural, and rural landscapes) is a patch mosaic of land-uses, in which spatial patterns emerge. While the function of a land-use patch is mainly determined by its land-cover composition, the structure and function of a landscape is a function of its (spatial) configuration as well as (non-spatial) composition. For example, the immense coverage of impervious surfaces may cause a UHI effect in urban areas (Arnfield, 2003); and $CO_2$ concentration increased along the rural-urban gradient in the Phoenix metropolitan area due to the intensity of traffic in urban center (Wentz et al., 2002). Urban ecosystems were found to respond promptly to the urban-induced environmental changes on the landscape scale (Ziska et al., 2004; Shen et al., 2008). Information of landscape structure can be provided as an input dataset to HPM-UEM, or generated by land-use models (see the Appendix A1). In model application, the local environmental drivers (e.g., temperature, $CO_2$, etc.) can be generated by geospatial statistical modeling (e.g., see the development of climate datasets in Table 2) or regional climate/atmosphere model simulations (e.g., see the development of $CO_2$ dataset in Table 2). HPM-UEM allows users to attach socioeconomic variables such as human population size or fossil fuel consumption to landscape types. These variables can be used to drive empirical equations that model the urban-induced environmental changes (e.g., Zhang et al., 2012). Finally, if dynamic environment modeling is impossible, empirical parameters can be used to define anthropogenic environmental changes at the landscape level.

As defined by Wu and David (2002), a region is a mixture of landscapes, and characterized by climate, geomorphology, hydrology, soils, and vegetation at the regional scale. Grimm et al. (2008a) pointed out that "considering the biogeophysical and social influence on urbanization, biogeochemical cycles are likely to exhibit regional differences". It was expected that the nature and strength of feedbacks among landscape patterns and ecosystem functions would vary across the climatic, societal, and ecological settings that characterize strongly contrasting regions (e.g., an urbanized coastal region vs. an urbanized desert region, or a North American metropolitan area vs. an East Asian metropolitan area). Classifying urbanized regions based on both social and biogeophysical variables, therefore, could form the basis for continental-scale comparisons of urbanization and their resulting ecosystem responses (Grimm et al., 2008a). In correspondence to the regional socioeconomic background, the same land-use or landscape type in different region types can have different land-use structure or management regimes. For example, lawn irrigation intensity could differ dramatically between a desert metropolitan region and a forest metropolitan region.

All ecosystem processes in a region (patch) are controlled by its background biogeophysical properties. Some of the environmental constraints should be provided as model inputs (Table 2), while others (e.g., solar radiation and daylength) can be estimated by HPM-UEM (see Appendix for further details). The following sections describe how critical ecological processes for different hierarchical levels (Table 1), such as land-use management and disturbances, population dynamics and competition, and plant growth and canopy structure, were modeled in HPM-UEM.

### 2.2. Land-use and land management

Based on user defined land-use parameters (e.g., Table 3), HPM-UEM can simulate the ecological impacts of various disturbances and management regimes. Land-management parameters include the time (dates or intervals) and intensity of N fertilization (g N/m$^2$), irrigation, and mowing, pruning, or harvesting events (see Appendix for details). HPM-UEM then simulates the impacts of disturbances on vegetation and soil, based on parameters that prescribe how disturbances generate C and N fluxes from the biomass to the detritus pools and from the ecosystem to atmosphere. Specifically, these effects are assessed by the following equations:

$$\Delta B_o = -Dis_{fract} \times B_o \times (Dis_{ltrfl,o} + Dis_{harv,o} + Dis_{burn,o}) \quad (1)$$

$$\Delta Ltr = \sum_{o \in organs} (B_o \times Disturb_{ltrfl,o}) - Ltr \times (Dis_{decom,ltr} + Dis_{harv,ltr} + Dis_{burn,ltr}) \quad (2)$$

$$\Delta SOM = k_{transf,ltr} \times Ltr \times Dis_{decom,ltr} - SOM \times (Dis_{decom,SOM} + Dis_{burn,SOM}) \quad (3)$$

**Table 2**
Background environmental drivers and constrains for the study region.

| Inputs | Unit | Description | Methods and data sources used in the Phoenix Metropolitan Area study |
|---|---|---|---|
| Soil clay content | % | Biophysical base maps | Based on the 1-km resolution digital general soil association map (STATSGO map) developed by the US Department of Agriculture (USDA) Natural Resources Conservation Service (NRCS), while the texture information of each map unit was estimated using the USDA soil texture triangle (Miller and White, 1998; Miller et al., 2004) |
| Soil sand content | % | | |
| Soil silt content | % | | |
| Soil depth | m | | |
| Soil acidity | pH | | |
| Soil bulk density | g/cm$^3$ | | |
| Elevation map | m | Environ-mental drivers | Generated from the 7.5-min US Geological Survey (USGS) National Elevation Dataset (NED). Data available online: http://edcnts12.cr.usgs.gov/ned/ned.html |
| Aspect map | ° | | |
| Slope map | ° | | |
| Daily precipitation | mm | | We compiled climate datasets between 2000 and 2005 from 321 stations, included within the Arizona Meteorological Network (AZMET), Phoenix Real-time Instrumentation for Surface Meteorological Studies (PRISMS) Network, Maricopa County Automated Local Evaluation in Real-Time (ALERT) Weather Station Network, US Forest Service Remote Automated Weather Station (RAWS) Network, and Automated weather observation system of the National Weather Service/Federal Aviation Administration (NWS/FAA) (see Appendix Fig. A1). Daily (2000–2005) spatial maps of each climate factor were developed by a kriging interpolation with an automatic variogram fit (Haas, 1990) |
| Daily maximum temperature | °C | | |
| Daily minimum temperature | °C | | |
| Daily average temperature | °C | | |
| Daily mean relative humidity | % | | |
| $CO_2$ | ppmv | | Spatially explicit $CO_2$ concentration based on a transportation dataset and an empirical model developed by Wentz et al. (2002) |
| Annual nitrogen deposition ($NH_x$ and $NO_y$) | g N/m$^2$ y$^{-1}$ | | Dry deposition: Grossman-Clarke et al. (2005); wet deposition: Baker et al. (2001); ratio of $NH_x$-N:$NO_y$-N: Lohse et al. (2008) |

**Table 3**
Parameters that defines human management and disturbance in the Central Arizona-Phoenix ecosystem.

| Management | Treatments or environmental effects | Sources |
|---|---|---|
| Annual lawn fertilization | 7.5 g N/m$^2$ | Survey and experts' opinions; Milesi et al. (2005) |
| Irrigation of lawns and crops | Lawn and crop fields were irrigated so that their growth was not limited by water. According to former reports, we assumed that irrigation reduced daily maximum temperature by about 5 °C | Brazel and Johnson (1980); Hall et al. (2008) |
| Lawn mowing | $Thresh_{LAI}$ = 1.2; $Interv_{cut}$ = 10 day (see Section 4 in Appendix). Most of the clippings entered the litter pool ($Dis_{ltrfl}$ = 70%), while about 30% entered the product pool that decomposed in 1 year ($Dis_{harv}$ = 30%) | Survey and experts' opinions; Milesi et al. (2005) |
| Street tree pruning | Calibrating the pruning parameters so that NPP of street tree was reduced by 25%. Related parameters were set as $Thresh_{LAI}$ = 2.7; $Interv_{cut}$ = 30 days. Pruned leaf entered the product pool that decomposed in 1 year, while pruned stem entered the product pool that decomposed in 10 years | Martin and Stabler (2004); Nowak et al. (2002); model calibration |
| Urban tree irrigation | With annual precipitation of 200 mm, the climate of CAP would not support growth of trees without supplemental irrigation. We assumed that deep-rooted tree PFTs obtained water from the bottom soil layer where soil water was recharged by irrigation or water leakage of sewage systems. Related parameters were set as $Irrig\_layer$ = 6; $Thresh_{irrig}$ = 0.5; $Interv_{irrg}$ = 1 day | Experts' opinions; Martin and Stabler (2004); model calibration |
| Crop harvest | $Dis_{ltrfl,o}$=100% (where o∈{leaf, stem, root}; see Section 2.1); $Dis_{harv,reprod}$ = 100%; $Dis_{ltrfl,sto}$ = 50% and $Dis_{harv,sto}$ = 50% (where *sto* denotes the storage pools); $Dis_{burn,ltr}$ = 2%, $Dis_{Ngas.ltr}$ = 50%, $k_{transf,ltr}$ = 4% | Houghton et al. (1983); Houghton (2003); Experts' opinions |

$$\Delta Product = \sum o \in organs(B_o \times Dis_{harv,o}) + Ltr \times Dis_{harv,ltr} \quad (4)$$

where *B*, *Ltr*, and *SOM* (g/m$^2$) denote the vegetation biomass, the litter (including coarse, woody debris), and the soil organic matter (SOM) pools, respectively; *o* denotes the vegetation organs of all plants in the community: the leaves, roots, stems (for sapwood and heartwood), fine roots, storage tissues, and reproductive pools (flower and fruit). $Dis_{fract}$ is a parameter that determines the fraction of disturbed vegetation; $Dis_{ltrfl,o}$, $Dis_{harv,o}$, and $Dis_{burn,o}$ determine the fraction of organ *o* that entered the litter pool, product pool (Product; i.e., the harvested woody or crop products), or were burned, respectively. $Dis_{decom.ltr}$, $Dis_{harv,ltr}$, and $Dis_{burn,ltr}$ determine the fraction of the litter pools that entered the SOM pool, product pools, or were burned, respectively. $Dis_{decom,SOM}$ and $Dis_{burn,SOM}$ determine the fraction of SOM lost through decomposition and fire, respectively. $k_{transf,ltr}$ determines the fraction of decomposed litter C that becomes SOM (see the following discussions of HPM-UEM detritus C pools).

Decomposition and fire disturbances result in $CO_2$ emission ($CO2_{disturb}$; g C/m$^2$). The N of the burned organic matter is released either into atmosphere as $NO_x$ gas ($Nemis_{disturb}$; g N/m$^2$) or into the soil as $NO_3^-$ ($s_{NO3}$):

$$CO2_{disturb} = \sum_{o \in organs} (C_o \times Dis_{burn,o}) + LtrC \times (Dis_{burn,ltr} + k_{CO2.ltr}) \times Dis_{decom.ltr} + SOC \times (Dis_{burn,SOM} + k_{CO2,SOM} \times Dis_{decom,SOM}) \quad (5)$$

$$Nmin_{distrub} = \sum_{o \in organs} N_o \times Dis_{burn,o} + LtrN \times Dis_{burn,trn} + SON \times Dis_{burn,SOM} \quad (6)$$

$$Nemis_{disturb} = \sum_{o \in organs} (N_o \times Dis_{burn,o} \times Dis_{Ngas,o}) + LtrN \times Dis_{burn,ltr} \times Dis_{Ngas,ltr} + SON \times Dis_{burn,SOM} \times Dis_{Ngas,SOM} \quad (7)$$

$$\Delta s_{NO3} = Nmin_{distrub} - Nemis_{disturb} \quad (8)$$

where $C_i$ (g C/m$^2$) and $N_i$ (g N/m$^2$) denote the C and N of the consumed organic matter, respectively; $Nmin_{disturb}$ is the N mineralization (g N/m$^2$) due to fire disturbances; $Dis_{Ngas,o}$, $Dis_{Ngas,ltr}$, and $Dis_{Ngas,SOM}$ are parameters that determine the fractions of mineralized N (from biomass, litter, and SOM pools, respectively) that are released into the atmosphere as $NO_x$ gases.

### 2.3. Land-cover and the coupled C–N–water–energy processes

The land-cover (or the local ecosystem) is the hierarchical level where the biogeochemical processes involving the plant community, soil organisms, and their abiotic environments take place. Two land-cover types are treated differently in HPM-UEM: the Impervious Surface and the Pervious Surface. A land cover with pervious surface is composed of single or multiple populations of PFTs. All populations share the same soil water pools, detritus pools, inorganic N pools, and dissolved organic matter pools. On the land-cover level, the functions of the plant community, such as gross primary productivity (GPP), are calculated by aggregating the functions of each plant in the community. For simplification, HPM-UEM assumes an even-aged population structure for each PFT, while tracking the population density (*Density*, plant/m$^2$) dynamics on a daily time step. Plants in the even-aged population are "average individual plants" (AIP), whose number is updated whenever new seedlings are added to the population. Sitch et al. (2003) showed that this approach could significantly improve the computational efficiency while maintaining an acceptable accuracy in simulating ecosystem functioning. That is,

$$Func_{lc} = \sum_{i \in lc} Func_{p,i} = \sum_{i \in lc} [Func_i \times Density_i] \quad (9)$$

where $Func_{lc}$ and $Func_{p,i}$ are the functions of the land cover ($lc$) and the population of PFT $i$ in $lc$, respectively; $Func_i$ is the function of AIP that represents the population $i$.

In HPM-UEM, the vertical structure of an ecosystem is composed of two canopy layers, the overstory of tree crowns and the understory of grasses and shrubs. In order to simplify the energy partition process, HPM-UEM assumes that crowns of plants belonging to the same canopy level do not overlap. Incipient solar radiation passes through and is partitioned among the overstory canopy, the understory canopy, and the soil surface, in sequence (See Appendix Fig. A2). Precipitation may also be intercepted by the two canopy layers, with the rest either lost by evapotranspiration and runoff, or partitioned among the multiple soil layers. Depending on the user's choice, the model may have two or more layers of soil water pools. In our case study in Phoenix, six soil layers were identified (in a top-down sequence to a total depth of 1 m), having depths of 0–10 cm, 10–20 cm, 20–40 cm, 40–60 cm, 60–80 cm, and 80–100 cm. The biogeochemical processes of C and water were coupled through energy-balance processes (See Appendix Fig. A1), while the C and N processes were coupled through the stoichiometry of plant organs and SOM. Detailed descriptions of how HPM-UEM models the radiation transmission and energy partitioning, daily water balance, and dynamics of the detritus C and soil inorganic N pools can be found in the Appendix. The following sections focus on the biogeochemical processes of impervious surfaces, population dynamics, and root competition for soil water.

#### 2.3.1. Modeling the biogeochemical processes of impervious surface

An impervious surface (*Impvs*) has no vegetation cover and stable soil C pools sealed by the impervious surfaces ($C_{Impvs}$). Following Cannell et al. (1999), the default value of $C_{Impvs}$ was set to 1 kg/m$^2$. Only the daily balances of the water and the N on the impervious surface were affected by environmental factors such as precipitation (*Ppt*, mm/day), the potential evapotranspiration rate (*Evap*, mm/day), and the N deposition rate (*Ndep*; g N/m$^2$/day):

$$\left.\begin{aligned} \Delta W\_impv &= Ppt - Evap - Srun \\ \Delta N\_impv &= Ndep - Nloss \end{aligned}\right\} \quad (10)$$

where *W_impv* (mm) and *N_impv* (g N/m$^2$) denote the water and N storage on the impervious surfaces respectively; *Evap* (mm/day) is the evaporation rate; *Srun* (mm/day) is the daily surface water runoff; *Nloss* is the N loss as gas or runoff.

$$Evap = PET \quad (\text{if } PET \le W + Ppt); \qquad \text{or}$$
$$Evap = W + Ppt \quad (\text{if } PET > W + Ppt) \quad (11)$$

where *PET* (mm/day) is the daily potential evapotranspiration, which is estimated using a Penman–Monteith approach (Wigmosta et al., 1994). An assumption related to the energy balance is that all snow falls onto the impervious surface melts instantly. To calculate the energy balance, the albedo of the urban impervious surface should be provided as parameters. The default value is 0.12, which is the mean of the roof (0.16) and road (0.08) as estimated by Oleson et al. (2008):

$$Srun = Ppt + W - Evap - W\_impv_{\max} \quad (\text{if } Ppt + W - Evap > W\_impv_{\max}) \quad (12)$$

where $W\_impv_{max}$ (mm) is the water retention capacity of the impervious surface. Following Brater (1968) the default value of this parameter is 0.56 mm.

$$\left.\begin{aligned} Nloss &= (Ndep + N\_impv) \times Srun/(Ppt + W - Evap) \quad (if\ Srun > 0) \\ Nloss &= Ndep + N\_impv - (W\_impv_{\max} \times Ncon\_impv_{\max}) \\ &\quad (if\ Srun \le 0 \& Ndep + N\_impv > N\_impv_{\max}) \end{aligned}\right\} \quad (13)$$

where $Ncon\_impv_{max}$ (g N/L) is the maximum N concentration in the water on the impervious surface.

#### 2.3.2. Population dynamics

If information about the vegetation composition of the land-covers is not available, HPM-UEM simulates the processes of competition and succession with its dynamic vegetation module. Constrained by bioclimatic limitations, different PFT populations may coexist in an ecosystem, competing for light, water, and nutrients. When data on the composition of vegetation is available, HPM-UEM switches to a static vegetation mode, which has a much higher computational efficiency. In either mode, the population density of a PFT is determined by the balance between plant establishment rate (*Estab*, plant/m$^2$) and plant mortality rate (*Mort*, plant/m$^2$).

$$\Delta Density_i = Estab_i - (Mort_{bioclim,i} + Mort_{light,i} + Mort_i) \times Density_i \quad (14)$$

where $Mort_{bioclim,i}$ (0–1) is the mortality rate caused by climatic stress, which is estimated using the bioclimatic model developed by Sitch et al. (2003). When the static mode is activated, or if the land-cover is a monoculture ecosystem (e.g., plantation), $Mort_{bioclim,i}$ is set to 0. $Mort_{light,i}$ (0–1) is the mortality rate due to light competition; and $Mort_i$ (0–1) is the daily background mortality rate of the plant.

The total biomass of new seedlings is added to the population of PFT $i$, and both the $Density_i$ and biomass of AIP$_i$, are modeled as:

$$\left.\begin{aligned} Density_{i,t} &= Density_{i,t-1} + Estab_i \\ B_{i,t} &= (B_{i,t-1} \times Density_{i,t-1} + B_{sdl,i} \times Estab_i)/Density_{i,t} \end{aligned}\right\} \quad (15)$$

where $t-1$ denotes the value of the last time-step, and $t$ denotes the updated value. $B_{i,t}$, $B_{i,t-1}$ a and $B_{sdi,i}$ (g/(m$^2$ plant)) are the biomass of the updated AIP, original AIP, and individual seedling, respectively. Seedlings can only be established in spaces not shaded by the canopy of the population $i$ and the canopy layer above (e.g., canopies of woody PFTs are always above canopy of grass PFTs):

$$Estab_i = Density_{sdl,i} \times (1 - FPC_c) \tag{16}$$

where $Density_{sdl,i}$ (number of seedlings/m$^2$) is a PFT-specific parameter that determines the mean seedling density in an open space; $FPC_c$ is the foliage projective coverage (FPC) of the canopy $c$. If $i \in overstory$, $c$ refers to the overstory; otherwise, $c$ includes both the overstory and understory. $FPC_c$ is the aggregated $FPC$ of all populations that belong to canopy $c$. The $FPC$ of population $i$ ($FPC_{p,i}$) is calculated from the $FPC$ of its AIP and crown area:

$$FPC_c = \sum_{i \in c} FPC_{p,i} = \sum_{i \in c} (FPC_i \times CA_{p,i}) = \sum_{i \in c} [FPC_i \times (CA_i \times Density_i)] \tag{17}$$

where $CA_{p,i}$ (m$^2$/population) is the crown area of population $i$. $FPC_i$ and $CA_i$ (m$^2$/crown) are the FPC and the crown size of the AIP $i$, respectively.

Following Sitch et al. (2003), when the aggregated FPC of an ecosystem exceeds the maximum value $FPC_{max} = 0.95$, the community is stressed by a light deficit. The mortality due to light competition is estimated as:

$$Mort_{light,i} = \frac{FPC - FPC_{\max}}{FPC} \tag{18}$$

Following Prentice et al. (1993), the background mortality rate is inversely related to the growth efficiency rate ($greff$), which depends on the C balance of the vegetation in the previous 365 days:

$$greff_i = \sum_{t=d-365}^{d} \frac{NPP_{t,i} - LTRFL_{t,i}}{VEGC_i} \tag{19}$$

where $NPP_{t,i}$ (g C/(plant day)) is the daily net primary productivity, $LTRFL_{t,i}$ (g C/(plant day)) is the daily litter fall rate, and VEGC (g C/plant) is the vegetation C of the AIP.

### 2.3.3. Root competition for soil water

Water extracted from soil by plant roots supports transpiration. To estimate water uptake from soil layer $n$ by each PFT population $i$, HPM-UEM first estimates the water demand for potential transpiration of the plant ($Ptran_i$, mm/day). Driven by the remaining leaf-absorbed shortwave energy, $Ptran_i$ is calculated using the Penman–Monteith approach, where canopy resistance ($r_c$) is largely controlled by stomatal conductance, which is related to photosynthesis. Photosynthesis is controlled by the leaf-absorbed PAR (i.e., $Rad_{abs,\,PAR}$), ambient $CO_2$ concentration, and environmental factors such as temperature and water potential of the foliage (see Appendix for details).

Once the $Ptran_i$ of the entire plant is determined, HPM-UEM will estimate the amount of water that needs to be extracted from each soil layer ($n$) by the root systems of the PFT $i$ ($Ptran_{i,n}$, mm/day). To account for water-stress compensation (i.e., water stress in one part of the root zone can be compensated by enhanced water uptake from other, wetter parts), HPM-UEM assumes that the water demand (i.e., $Ptran_{i,n}$) is proportional to a weighted stress index, which is a function of both relative root density ($Rootfract_{i,n}$, 0–1) and available water ($AVW_{i,n}$, mm; see Appendix for details).

$$\left.\begin{aligned} Ptran_{i,n} &= Weight_{i,n} \times Ptran_i \\ Weight_{i,n} &= \frac{Rootfract_{i,n}^{\alpha} \times AVW_{i,n}}{\sum_{n=1}^{N} Rootfract_{i,n}^{\alpha} \times AVW_{i,n}} \end{aligned}\right\} \tag{20}$$

in which we set $\alpha$ to 1.0, a value between the theoretical estimation of >1.1 (van der Ploeg et al., 1978; Passioura, 1985) and the experimentally derived value of 0.5 (Ehlers et al., 1991).

The vertical distribution of the root system through the soil layers was calculated based on the asymptotic equation $Y = 1 - \beta^d$ (Gale and Grigal, 1987), where $Y$ is the cumulative root fraction (0–1) from the soil surface to the depth $d$ (in centimeters), and $\beta$ is the fitted extinction coefficient taken from Jackson et al. (1997). Therefore, $Rootfract_{i,n} = Y_{i,n} - Y_{i,n-1}$.

Next, HPM-UEM estimates the actual transpiration rate ($Tran_{lc,n}$, mm/day) from layer $n$ by comparing its AVW and the water required to support the potential transpiration of vegetation in the land-cover ($Tran_{lc,n} = \sum_{i \in lc} Tran_{lc,n}$). In the dynamic vegetation mode (refer to Section 2.3.2), populations of different PFTs will compete for the soil water. The water available to plant $i$ (i.e., $AVW_{i,n}$) is linearly proportional to the competitiveness of its root in the soil layer; the competitiveness of root $i$ in the soil layer n ($Rtcomp_{i,n}$) is linearly proportional to its active surface area ($Rtsurf_{i,n}$, m$^2$):

$$\begin{aligned} Tran_{lc,n} &= \min(AVW_{soil,n}, Ptran_{lc,n}) \\ AVW_{i,n} &= Rtcompi_{i,n} \times AVW_{soil,n} \\ Rtcompi_{i,n} &= 100\%(\text{in Static Vegetation Mode}) \\ Rtcompi_{i,n} &= \frac{Rtsurf_{i,n}}{\sum_{i \in lc} Rtsurf_{i,n}} (\text{in Dynamic Vegetation Mode}) \\ Rtsurf_{i,n} &= C_{root,i} \times Density_i \times Rootfract_{i,n} \times SRL_i \times (\pi \times D_{root,i}) \end{aligned} \tag{21}$$

where $C_{root,i}$ (g C/plant) is the fine-root carbon density of the PFT $i$; $Density_i$ (individuals/m$^2$) is the population density of PFT $i$; $SRL_i$ (m/g C) is the specific root length; $D_{root,i}$ (m) is the mean diameter of fine roots of PFT $i$. The PFT-specific parameters of $SRL$ and $D_{root}$ are derived from Jackson et al. (1997). Finally, the actual transpiration rate of the PFT $i$ ($Tran_i$, mm/day) and the limitation of water on the plant's GPP ($f_{gpp,water,i}$, see the descriptions of photosynthesis and plant productivity in Appendix) are estimated as:

$$\left.\begin{aligned} Tran_{i,n} &= Ptran_{i,n} \times (Tran_{lc,n}/Ptran_{lc,n}) \\ Tran_i &= \sum_{n=1}^{N} tran_{i,n} \\ f_{gpp,water,i} &= tran_i/Ptran_i \end{aligned}\right\} \tag{22}$$

## 2.4. Individual plant level

An individual plant is composed of four structural organs: leaves, fine roots (frt), sapwood (swd), heartwood (hwd; only in woody PFT), and reproductive organs (reprod). In woody PFT, swd and hwd together compose the stem (aboveground part) and coarse root (crt; belowground part). HPM-UEM assumes a fixed ratio ($\eta_{stmcrt}$) between the stem and the coarse root, and fixed C:N ratios for the organs of a certain PFT. HPM-UEM also has internal storage pools for C ($C_{store}$) and N ($N_{store}$) for unallocated photosynthate and mobile N. Description of plant physiological processes such as photosynthesis, maintenance respiration, tissue turnover, and N uptake are found in Appendix. Following sections focus on the allocation of photosynthate.

The allocation routine considers the basic functional constraints between the different tree parts, with nitrogen allocation following

carbon allocation, using mostly empirical principles. First, a fraction ($k_{gpp\_repd}$, ranging from 5% to 35%) of the photosynthate is allocated to the reproductive pool (Larcher, 1980). Then, the remaining photosynthate is added to $C_{store}$ and will be allocated to different live, structural organs (i.e., leaf, sapwood, and fine root). Non-live tissues such as heartwood will not be changed by allocation. Following C allocation, N is partitioned so as to maintain constant C:N ratios of each organ. If the demand for N exceeds $N_{store}$, plant growth is limited and excessive C is added to $C_{store}$. In this case, a fraction of the increased $C_{store}$ ($\Delta C_{store} = GPP_{excs}$ in Appendix) enters the soil as dissolved organic C, stimulating microbial processes and enhancing the rate of N mineralization (Schimel and Weintraub, 2003; Montaño et al., 2007).

C allocation to the live, structural organs takes place on a daily time step to maintain the form of the plant (i.e., the ratios of C among live structural organs). A non-woody PFT is assumed to have a fixed form throughout its lifespan, while the form of a woody plant is updated annually, based on three constraints: (1) foliage area is assumed to be linearly proportional to sapwood area at breast height; (2) the ratio of foliage and fine root C mass is fixed; (3) the allometric relationship between diameter at breast height (DBH, meter) and woody C mass is fixed. When the form of a woody plant is updated, stem diameter, crown properties, and biomass (C pool size) of its organs are updated (see Appendix for details). Crown size (CA, $m^2$/crown) of plant $i$ is related to its DBH (Zeide, 1993):

$$CA_i = k_{cr1} \times DBH_i^{k_{cr2}} \tag{23}$$

where $k_{cr1}$ (default value = 100) and $k_{cr2}$ (default value = 1.6) are empirical parameters (Sitch et al., 2003). The LAI of crown $i$ ($LAI_i$), sunlit crown ($LAI_{i,sunlit}$), shaded crown ($LAI_{i,shade}$), and FPC are then calculated as:

$$\left.\begin{aligned} LAI_i &= LA_i/CA_i \\ LAI_{i,sunlit} &= 1 - \exp(-LAI_i) \\ LAI_{i,shade} &= LAI_i - LAI_{i,sunlit} \\ FPC_i &= 1 - \exp(-0.5 \times LAI_i) \end{aligned}\right\} \tag{24}$$

## 3. Model implementation

### 3.1. Study region

We implemented and tested the HPM-UEM with data from the Central Arizona-Phoenix (CAP) Long-Term Ecological Research (LTER) site (central latitude/longitude: 33.52°/−112.08°; mean elevation: 340 m; Fig. 2a). The study area (6608 $km^2$) includes the Phoenix (AZ, USA) metro area (2577 $km^2$), along with surrounding agricultural land (925 $km^2$) and desert (3105 $km^2$), with a population size of more than 4 million people (US Census Bureau, 2010). Annual precipitation of the region is ~180–210 mm divided approximately evenly between winter and summer rain seasons. Mean annual temperature is ~22 °C, with hot summers and mild winters. Native vegetation is characterized by desert shrub/scrub communities (Grimm and Redman, 2004). Urban and developed land is occupied by large areas of either cultivated grass and broadleaf trees or desert-like landscaping with drought-tolerant shrub species and gravel ground cover. More details of the biogeophysical and socioeconomic settings of the Phoenix metropolitan region are found in Wu et al. (2003), Grimm and Redman (2004), Martin et al. (2004), and Jenerette et al. (2007).

### 3.2. Model parameterization and implementation

Physiological parameters for major PFTs in the Phoenix metropolitan area can be found in Table A1 of Appendix. We developed a land-use map of the study region (Fig. 2a) by combining two land-use classifications: the classification system for the 200-point survey of the CAP landscape (Grimm and Redman, 2004), and the land-use map of Phoenix, developed by Buyantuyev et al. (2010). In the 200-point survey, a dual-density, tessellation-stratified random sampling design was applied to characterize the spatial heterogeneity of the Phoenix landscape. This design, which established 204 sampling points, each randomly selected within a grid cell of 5 km × 5 km (with outlying points established in every third grid cell, hence the dual density), provided detailed information on the land-use structure of Phoenix (Fig. 2b).

In total, twelve land-use types were identified: agricultural land, large patches of cultivated grass for recreational land-use (e.g., golf courses), fluvial sediments/bare canal, commercial/industrial areas, transportation areas, undisturbed deserts, construction/vacant areas, mesic residential areas, xeric residential areas, riparian zones, water, and other vegetated areas. Except for the water areas, all land-uses were considered in the model simulations, and information of their land-use structure (i.e., the land-cover composition) was generated based on the results of the 200-point survey (Fig. 2b). According to the survey, we identified seven land-cover types in the study region: bare ground, impervious surfaces, arid grassland ecosystems, lawns, urban forests, cropland, and arid shrub/scrub communities. Each land cover was occupied by one or more of the following PFTs: C3 grass, C4 grass, managed turf grass, desert shrubs/scrub, deciduous broadleaf trees, and C3 crops, which is the dominant crop type in the region (Baker et al., 2001). We did not consider the needle leaf tree PFT, which account for less than 15% of Phoenix's tree biomass, according to the 200-point survey (Hope et al., 2005).

The simulation spans the period from 2000 to 2005. Spatial datasets of environmental inputs (Table 2) defined the background biogeophysical constraints or environmental drivers in the study region. Because spatial patterns of environmental drivers such as $CO_2$, temperature, and N deposition rate were available for our study region (Table 2), we need not provide parameters that indicate how urbanization-induced changes (e.g., UHI, $CO_2$ dome) modified the spatial pattern of background environment in urban landscape (see Section 2) in this study. On the land-use hierarchical level, structures and environments of land-cover types were modifiable due to human land-management practices or disturbances (Table 3). HPM-UEM was first run to an equilibrium state using a mean climate dataset to develop the simulation baseline for C, N, and water pools. Then a 90-year spin-up simulation was conducted using climate data with trends removed to eliminate noise caused by a shift in the simulation from the equilibrium to the transient state. This approach subtracted the best-fit line from the transient climate dataset, retaining only the trend fluctuations. Such a dataset is required for stabilizing the simulation before entering the transient mode. Finally, driven by daily transient climate datasets, HPM-UEM simulated annual C fluxes and pool sizes from 2000 to 2005. Based on the 2005 outputs, we analyzed the spatial pattern of C storage, NPP, and the contribution of different land-use types and land-cover types to the C storage and productivity of the study region.

### 3.3. Model evaluation

Using the Phoenix metropolitan landscape as a case study, we conducted model validations at multiple scales. First, we compared the model-simulated daily GPP and daily net ecosystem exchange (NEE = NPP − Rh) against the observations from several Ameriflux sites (http://public.ornl.gov/ameriflux/) that represented major PFTs of the Phoenix ecosystem and were close to the study region (see Appendix for details). Parameters for each PFT are provided in Appendix. Second, we compared the modeled C density of different land-use types against reports from empirical studies based on the

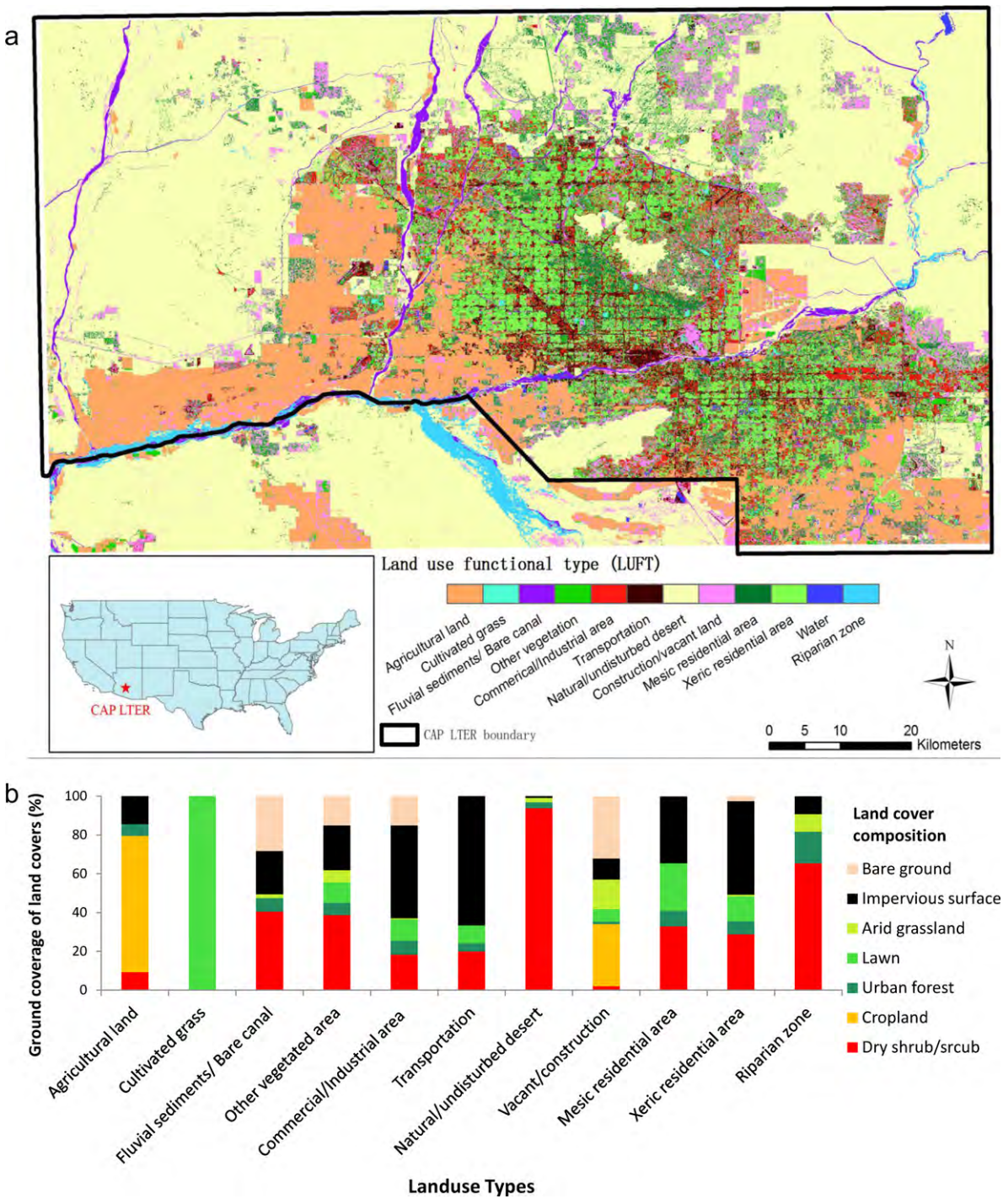


**Fig. 2.** Hierarchical land structure of Phoenix, AZ. (a) Land-use composition of the urban landscape (Buyantuyev et al., 2010) and (b) land-cover compositions of land-use functional types based on the 200-point survey of the Central Arizona-Phoenix Long-term Ecological Research project (CAP LTER, Grimm and Redman, 2004).

CAP LTER's 200-point survey (Grimm and Redman, 2004; Jenerette et al., 2006; Kaye et al., 2008). Third, to evaluate the model's ability to simulate the spatial pattern of the Phoenix landscape's ecosystem functions, we compared the modeled NPP against the primary productivity estimated as annual accumulated NDVI × PAR by Buyantuyev and Wu (2009). Finally, to evaluate the model's capacity to capture temporal variation in ecosystem function, we compared the modeled annual NPP ($gC/m^2$) against the annual accumulation of NDVI × PAR of the Phoenix landscape from 2002 to 2005 (Buyantuyev and Wu, 2009).

To evaluate model performance, we further conducted sensitivity analysis by systematically changing the values of the environmental drivers, such as temperature, precipitation, $CO_2$ concentration and annual N deposition rate (Fig. 3a). To evaluate the impact of spatial pattern on the carbon balance of different land-use types, we compared modeled C storage to the results from a non-spatial scenario where (spatially) averaged environmental factors of the study region were used to drive the model. Finally, to evaluate the importance of including the land-use or the landscape hierarchical levels in the HPM-UEM,

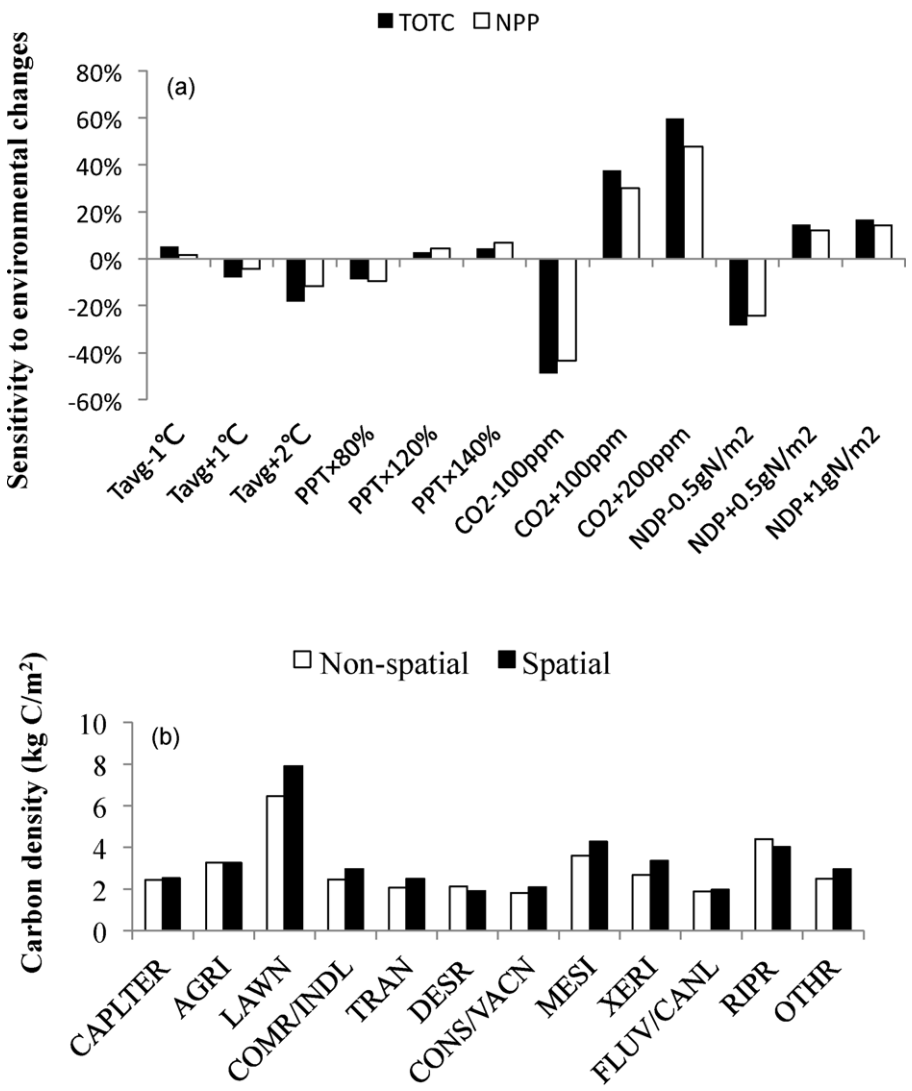


**Fig. 3.** Sensitivities of modeled C dynamics to (a) various environmental changes (sensitivity = $(Value_{changed} - Value_{control})/Value_{control} \times 100\%$), and (b) the spatial pattern of CAP LTER. Tavg: daily mean temperature, PPT: precipitation, $CO_2$: $CO_2$ concentration, NDP: annual nitrogen deposition. LAWN: lawn/cultivated grassland, XERI: xeric residential area, MESI: mesic residential area, COMR/INDL: commercial/industrial area, DESR: native or undisturbed desert, AGRI: agricultural land, TRAN: transportation, FLUV/CANL: fluvial sediments/bare canal, CONS/VACN: construction/vacant area, RIPR: riparian zone, OTHER: other vegetated area.

we conducted two model experiments by removing each of the two levels (and the related processes, e.g., land-use managements or urban-induced environmental changes) from the model structure.

### 3.3.1. *Carbon fluxes*

The modeled daily carbon fluxes (both GPP and NEE) were significantly correlated with observations for all PFTs (Fig. 4). The correlation strength (or R-squared values) of GPP was higher than that of NEE. The primary productivity of an ecosystem responds promptly to short-term environmental changes, while NEE is also controlled by ecosystem respiration rates, which are related to long-term dynamics of vegetation biomass and soil C storage. Because historical climate and atmospheric data were lacking for Ameriflux sites, we were unable to replicate the long-term environmental changes of the validation sites. The base-line statuses of model simulations were developed by running HPM-UEM until an equilibrium state was reached, using environmental datasets of the first validation year (Table A2 in the Appendix). Such an approach was not able to reflect the legacy effects of historical environmental changes on NEE. Nevertheless, the temporal pattern of the simulated NEE generally matched observed C fluxes as shown in Fig. 4b.

Carbon flux measurements at the land-use scale were not available. The predicted soil and vegetation C densities of various land-use types, however, generally agreed with those reported in several empirical studies (Fig. 5a). On the landscape scale, the spatial pattern of simulated productivity was significantly correlated to the primary productivity maps derived from remote-sensing images (Buyantuyev and Wu, 2009; Fig. 5b). The temporal pattern of annual productivity in the Phoenix landscape was also highly correlated with the remote-sensing based estimations (Fig. 5c), indicating that HPM-UEM can accurately simulate an ecosystem's response to climate changes.

In the Phoenix landscape case study, we found that HPM-UEM responded promptly to changes in atmospheric $CO_2$ concentration, N deposition, precipitation and temperature, as well as the spatial configuration of the landscape (Fig. 3). A sensitivity analysis indicated that spatial configuration affected the C storage of urban land-uses. It also indicated that the modeled ecosystem productivity and C storage were generally positively correlated to environmental factors except for temperature (Fig. 3a).

*3.3.2. Multi-scaled analysis of the carbon storage in the Central Arizona-Phoenix (CAP) landscape*

HPM-UEM provides a tool to comprehensively analyze the structure and dynamic of urban C pools and their responses to environmental controls across multiple scales. According to our model simulation, the C storage of the 6608 km$^2$ CAP metropolitan area was about 16.7 Tg C, where soil organic carbon accounted for nearly 74% of the C storage, while vegetation C accounted for another 21%. The remaining C was stored in litter or product pools (such as harvested crops or pruned branches or leaves). Carbon storage of the three landscape types – agricultural lands, native deserts, and the Phoenix metro area, were about 2.9 Tg C, 5.9 Tg C, and 7.9 Tg C, respectively. We found high spatial heterogeneity in the distribution of the C pools and fluxes (Fig. 6). The Phoenix metro area has relatively high C density, especially in the northern city, where mesic residential area and large patches of golf courses were found. Relatively high NPP was found in the agricultural lands located to southwestern and southeastern of the city (Fig. 6). Further analysis at the land-use scale revealed C storage distribution across the CAP landscape among different land-use types (Fig. 7). We found that the undisturbed deserts, which covered about 47% of the study area, only accounted for about 26% of its NPP. In contrast,

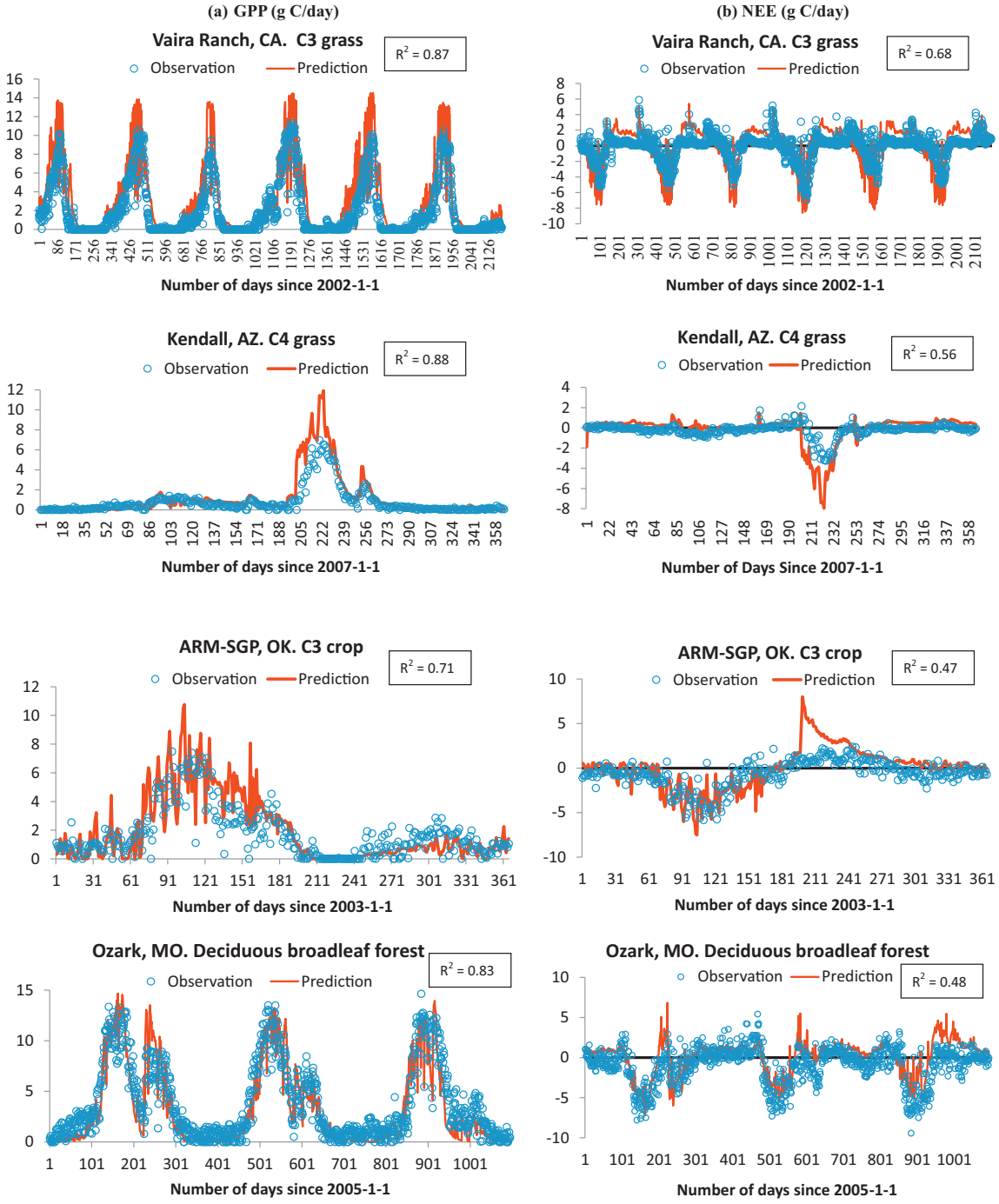


**Fig. 4.** Comparing model simulated carbon fluxes against observed GPP (panel (a)) and NEE (panel (b)) from six Ameriflux sites (public.ornl.gov/ameriflux) that represent the major PFTs of the CAP ecosystem and are located close to the study region. The $R^2$ values indicate the coefficient of determination between the observations and the model predictions.

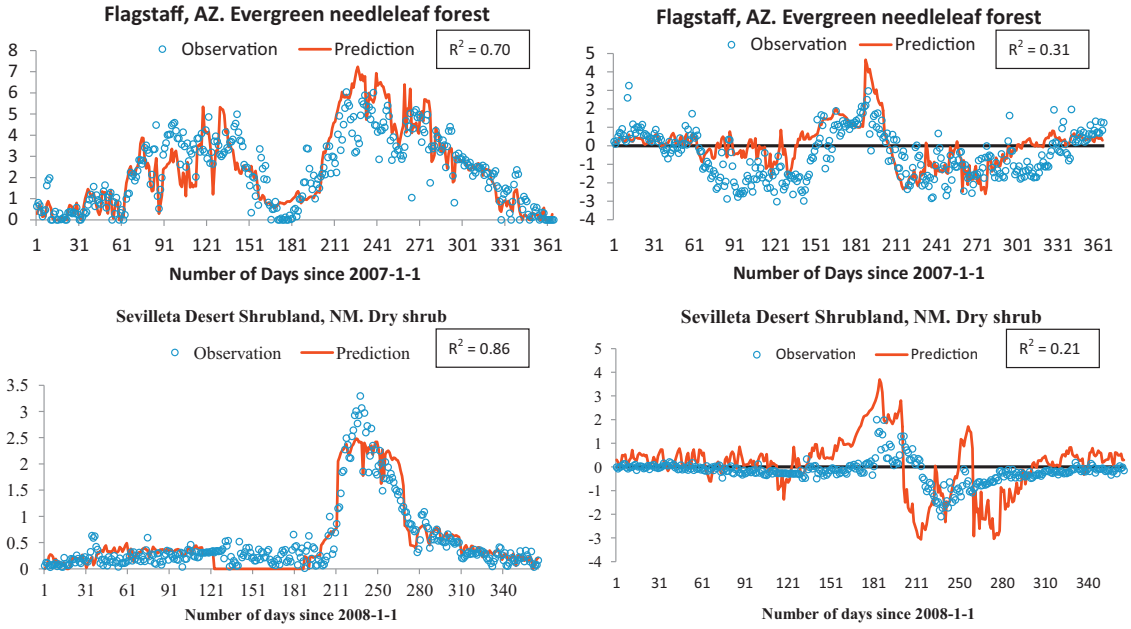


**Fig. 4.** (*Continued*).

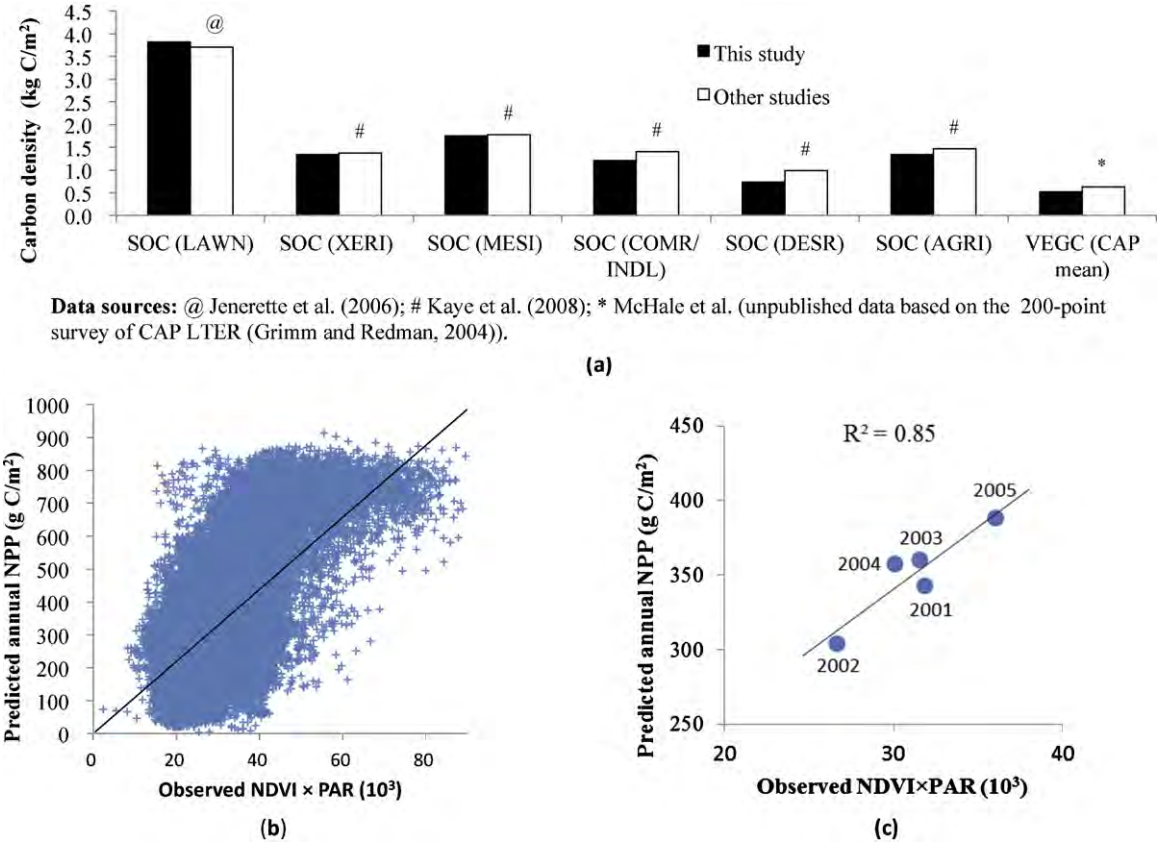


**Fig. 5.** Model evaluation at land-use and landscape scales. (a) Comparing modeled soil organic carbon (SOC) of different land-use functional types and vegetation carbon density (VEGC) in the CAP ecosystem against reported values from field observations (LAWN: lawn/cultivated grassland, XERI: xeric residential area, MESI: mesic residential area, COMR/INDL: commercial/industrial area, DESR: undisturbed desert, AGRI: agricultural land); (b) pixel by pixel comparison of the modeled annual NPP (1 km × 1 km resolution spatial datasets) against the remote-sensing-derived annual NDVI × PAR maps for the CAP ecosystem. Annual accumulated NDVI × PAR was used as approximation of the net primary productivity (NPP) of the CAP ecosystem (Buyantuyev and Wu, 2009). (c) Comparing the temporal pattern of the modeled annual NPP against the annual NDVI × PAR values between 2001 and 2005. NDVI: normalized difference vegetation index; PAR: photosynthetic active radiation.

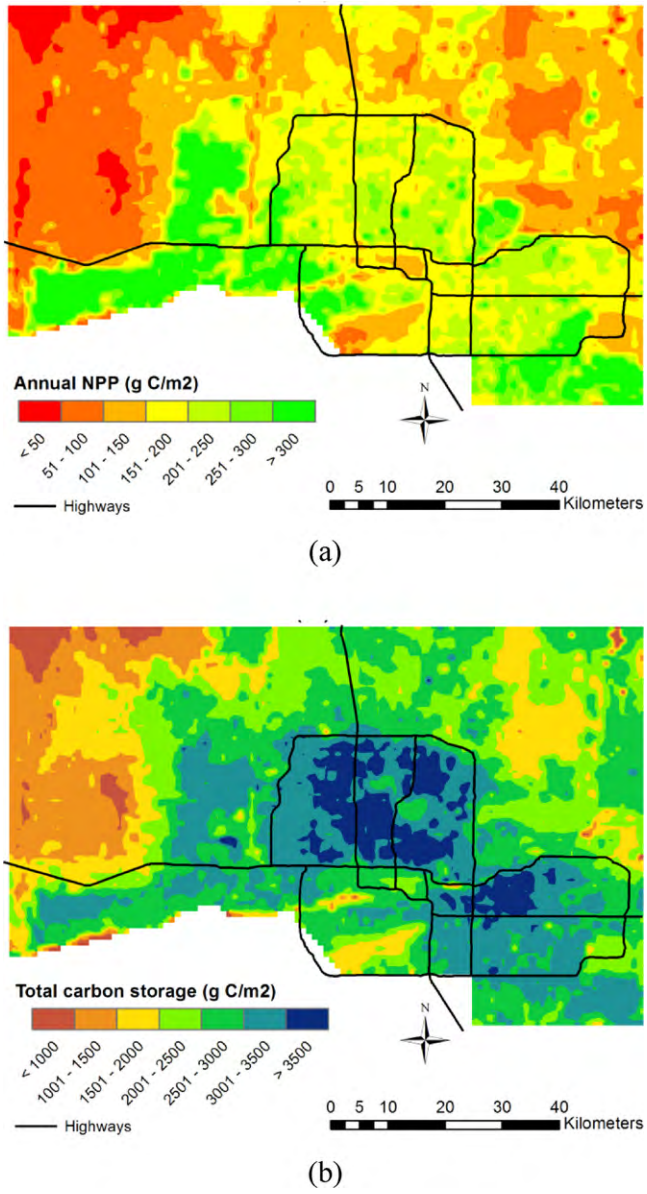


**Fig. 6.** Model simulated spatial patterns of (a) the annual net primary productivity (NPP) and (b) ecosystem carbon storage in the study region. The Phoenix metro area is delineated by the highway network.

agricultural land covered 17% of the study region, but accounted for about 31% of its NPP (Fig. 7a). We also found that the cultivated grassland such as golf courses, which only covered 0.3% of the study region, accounted for 1.5% of the regional NPP and 1% of the regional C storage. The disproportionate contribution of the lawns or cultivated grassland to the regional C cycle was related to their extraordinarily high productivity (Kaye et al., 2005) and C density, compared to other land-use types (Fig. 7b).

On the land-cover hierarchical scale, we found that although the arid shrubland communities covered 54% of the study region, croplands had the largest productivity (37% of total NPP). Urban forests (i.e., all the trees in the Phoenix landscape), which only covered 4% of the total area, accounted for 27% of the C storage (Fig. 8a). This was due to the high C density of the urban trees (Fig. 8b). Despite their small coverage, urban lawns were found to be an important contributor to the productivity and carbon storage of the urban landscapes in our study.

## 4. Discussion

### 4.1. Justification for including six hierarchical levels in HPM-UEM

It may be argued that urban ecosystem studies may not need to include so many land hierarchical levels (i.e., the land-cover, land-use, landscape, and region levels) that do not directly relate to ecological mechanisms. Former urban ecosystem studies (e.g., Trusilova and Churkina, 2008) considered two scales at most: the local ecosystem that is directly related to ecosystem mechanisms, and the landscape scale that addresses urban-induced environmental changes. HPM-UEM considers four urban land hierarchies because ecosystem functions are under the influences of multiple anthropogenic environmental controls on multiple scales, such as the regional climate/atmosphere changes, urban-induced environmental changes, and land-use management with associated microclimate effects. A hierarchical patch mosaic model that fully addresses the environmental changes at regional, landscape, and land-use scales is required to model the complex spatiotemporal pattern of urban climate, $CO_2$, N deposition, and land-use management. Furthermore, a hierarchical model structure can facilitate linking local ecosystem processes to land-use change and socioeconomic dynamics that work at the land-use, landscape, and regional scales (Jenerette, 2004) (see Appendix Fig. A1).

Our modeling experiments indicated that without addressing the landscape hierarchical level, HPM-UEM underestimated the C storage in the Phoenix metropolitan area by 17%. When the land-use hierarchical level and the related land-use management (Table 3) were excluded from the HPM-UEM, the C storage was underestimated up to 48%. In model applications, the highest simulation hierarchy should be determined according to the extent of the study areas and research questions (Wu, 1999). Limited by the extent of the CAP LTER area, the hierarchical level of region was not considered in the Phoenix case study. Previous urban research, however, proposed to consider a regional hierarchical level when conducting continental or global-scale urban ecosystem comparisons (Wu and David, 2002; Grimm et al., 2008a; see Section 2.2).

The importance of explicitly modeling the individual plant and population levels in a hierarchical ecosystem model was discussed in the "Introduction section". Considering these hierarchical levels is not only required for modeling common urban tree management such as pruning and selective harvesting/transplanting (Nowak et al., 2002; Martin and Stabler, 2004), but also important for addressing ecological processes such as energy partition (Yang et al., 2001), vegetation dynamics (Ziska et al., 2004; George et al., 2009), and biological invasion (Wang et al., 2011). Although vegetation succession was not simulated in this case study due to the lack of long-term environmental datasets, it by no means implies this is an unimportant process. The Phoenix case study was conducted solely for the purpose of model evaluation, thus the research objectives focused on model development rather than analyzing the Phoenix ecosystem. We tried to address the complex structure of the human-dominated landscape and the related ecosystem processes as completely as possible, so that HPM-UEM could be applied in a wide range of ecosystem studies from local to continental scales. With the object-oriented software engineering and the client/server interface structure (Booch, 1994), the model provides a framework to link ecosystem processes to the hierarchically organized urban land system and its underlying socioeconomic dynamics (see Appendix Fig. A1).

### 4.2. A more complete understanding of the C cycle in the Phoenix urban ecosystem

Urban landscapes are composed of multiple land-cover (or ecosystem) types with different functions (Wu and David, 2002).

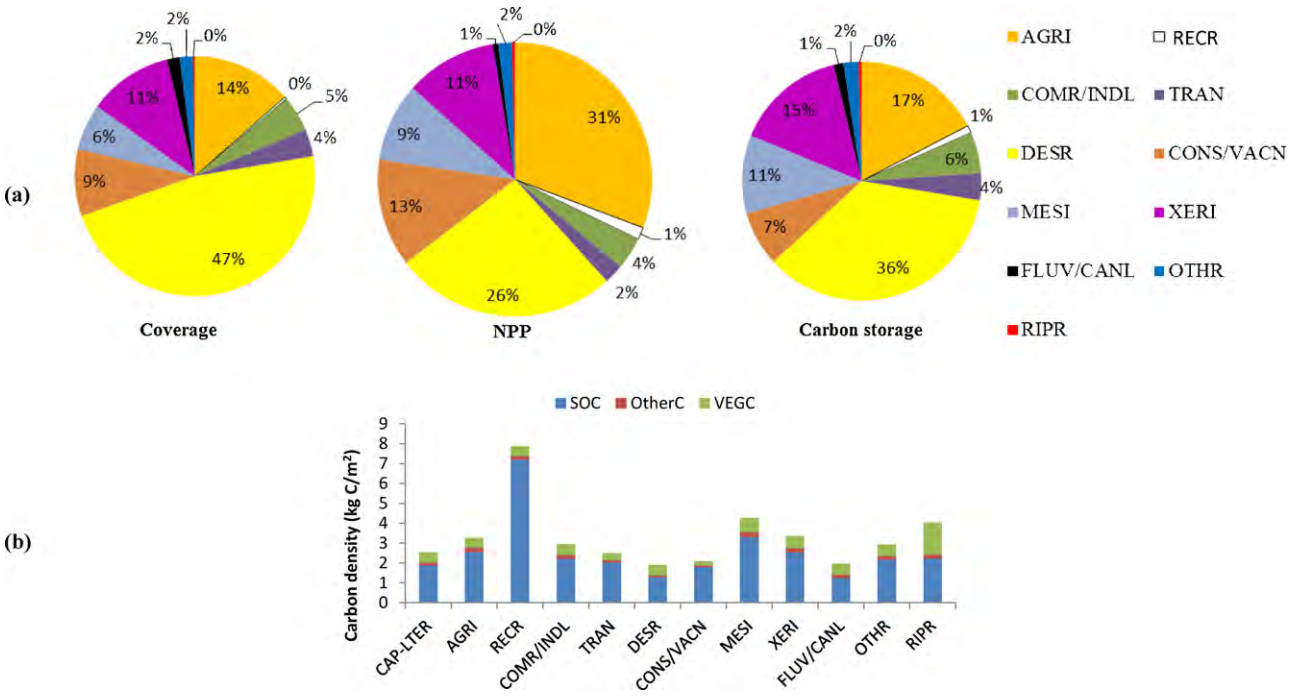


**Fig. 7.** Analyzing carbon balance at the land-use hierarchical level: (a) contribution of different land-use types to net primary productivity (NPP) and carbon storage of the study region; (b) carbon density of land-uses as simulated by HPM-UEM. VEGC: vegetation carbon; SOC: soil organic carbon; OtherC: carbon stored in litter, coarse woody debris, and product pools (such as harvested crops or clipped twigs/leafs by tree pruning); RECR: large patches of cultivated grass for recreational land-use (e.g., golf courses); XERI: xeric residential area; MESI: mesic residential area; COMR/INDL: commercial/industrial area; DESR: undisturbed desert; AGRI: agricultural land; TRAN: transportation; FLUV/CANL: fluvial sediments/bare canal; CONS/VACN: construction/vacant area; RIPR: riparian zone; OTHER: other vegetated area.

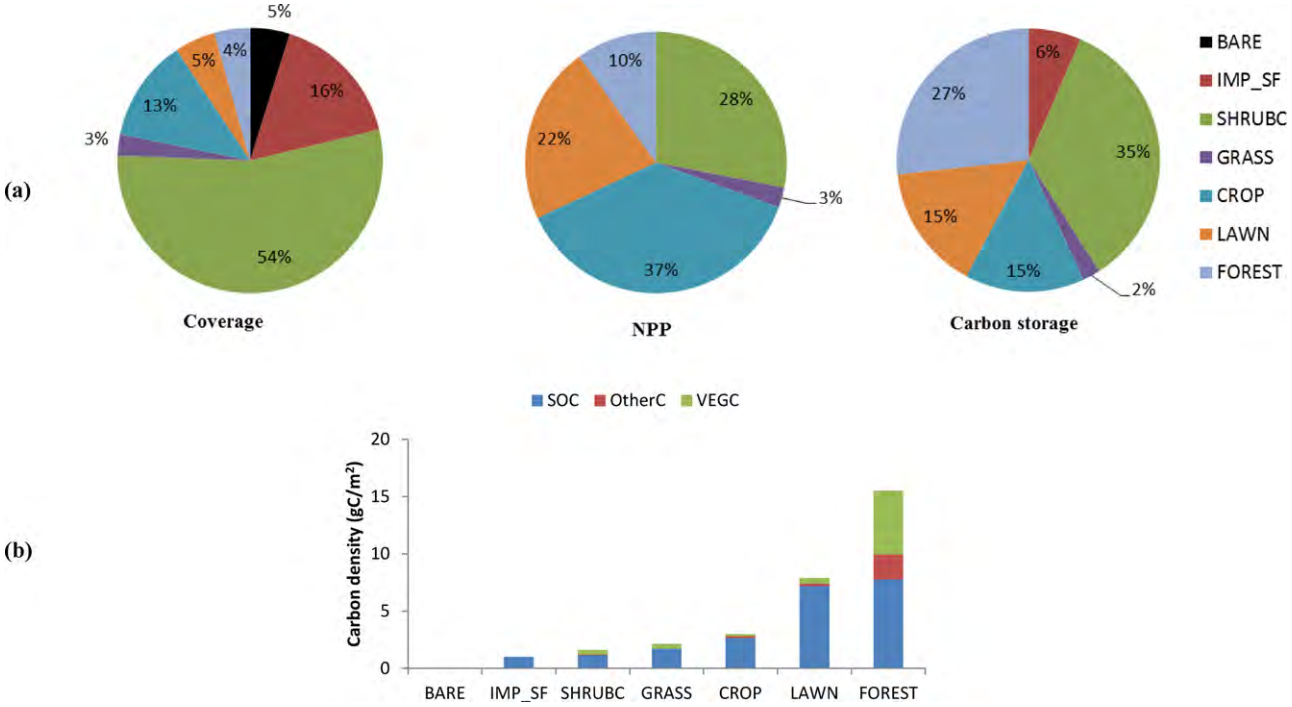


**Fig. 8.** Analyzing carbon balance at the land-cover hierarchical level: (a) contribution of different land-cover types to the net primary productivity (i.e., NPP) and carbon storage of the study region; (b) the carbon density of land-covers as simulated by HPM-UEM. VEGC: vegetation carbon; SOC: soil organic carbon; OtherC: carbon stored in litter, coarse wood debris, and product pools (such as harvested crops or clipped twigs/leafs by tree pruning); BARE: bare soil; IMP_SF: impervious surface; SHRUBC: arid shrub/scrub community; FOREST: urban forest, mainly composed of broadleaf deciduous trees.

Yet, they have been represented in many carbon cycles studies as a single land-cover type, such as cultivated land (e.g., VEMAP, Schimel et al., 2000), grassland (McGuire et al., 2001), or the dominant vegetation type in an area (Imhoff et al., 2004). Shen et al. (2008) used desert shrub/scrub community, which covered more than half of the Phoenix metropolitan region (Fig. 8), to represent the ecosystem in Phoenix, AZ. They estimated the annual aboveground NPP (ANPP) to be 38 g C/m$^2$, indicating a total NPP

of 61 g C/m$^2$ to 108 g C/m$^2$ (Barbour, 1973; Huxman et al., 1999). This value was close to our estimated shrub/scrub NPP (90 g C/m$^2$), but much lower than the NPP (175 g C/m$^2$) of the Phoenix ecosystem according to our study. Other studies, based on observations of urban lawn (Kaye et al., 2005) and forest (Nowak and Crane, 2002), suggested that urban ecosystems had high NPP and C density (Pouyat et al., 2007). However, the relatively small coverage of these land-covers limited their contributions to the overall C balance of the Phoenix's ecosystem (Fig. 8). As a desert city with low forest coverage (4%), vegetation C density of Phoenix, AZ was less than 5% of the value observed in Seattle, WA, a city with high (57%) forest coverage (Hutyra et al., 2011), highlighting the importance of land-cover composition in the C cycle of urban ecosystem. Our study, like a few empirical studies (Koerner and Klopatek, 2002; Pouyat et al., 2006; Hutyra et al., 2011), highlighted the distinct C dynamics among different land-covers (Fig. 8b), factors which should be taken into account in global and regional carbon-cycle modeling. The inventory approach used by those empirical studies (Koerner and Klopatek, 2002; Pouyat et al., 2006), however, completely relies on the availability of observational dataset, which is still relatively rare for urban ecosystems compared to other ecosystem types (Pickett et al., 2011). In contrast, because the basic ecological mechanisms are unchanged in an urban landscape, the process-based modeling approach in this study can make predictions for urban ecosystem based on the knowledge learned from long-term research on rural ecosystems (Niemelä, 1999). Furthermore, in comparison to empirical approaches, process-model like HPM-UEM can predict ecosystem responses to complex environmental changes due to urbanization, as was showed by the sensitivity analysis of this study (Fig. 5a) and other studies (Shen et al., 2008; Trusilova and Churkina, 2008). Unlike many previous studies that directly applied models (and sometime parameters) designed for rural ecosystems to urban ones, HPM-UEM explicitly addresses anthropogenic disturbances (e.g., UHI, lawn management) in each hierarchical level (Fig. 1), factors that were found to have important impacts on the biogeochemical cycles of urban ecosystem (Nowak et al., 2002; Martin and Stabler, 2004; Milesi et al., 2005). Compared with other urban ecosystem models, which only focus on C or water cycles, HPM-UEM fully couples energy, water, C, and N processes, and thus is able to address the important interactions among biogeochemical processes in urban landscapes (Pataki et al., 2011).

Among the urban carbon-cycle studies, spatial heterogeneity of urban landscapes was rarely taken into account (but see Hutyra et al., 2011). HPM-UEM is one of the few urban ecosystem models that explicitly address the spatial pattern of urban landscapes. Our sensitivity analysis (Fig. 3b) supported the assertion that the spatial pattern of an urban landscape affects ecosystem C balance (Alberti, 2010). According to the simulation results, the effects of spatial pattern accounted for about 4% of C storage in the region. Therefore, it is possible for policy makers to manage for specific ecosystem functions of urban landscapes, such as, C storage capacity, by altering the configuration as well as the composition of urban land-uses. Furthermore, when comparing the sensitivities of land-uses with the sensitivity of the CAP LTER region, we found that the effects of spatial configuration were more prominent on the land-use hierarchical level than on the landscape level (Fig. 3b). Similarly, when comparing C density in Fig. 7b and Fig. 8b, we found the differences among land-covers were much greater than the variation among land-uses. These findings are consistent with the hierarchy theory, which suggested that variations in ecological functions at lower hierarchical levels may be "smoothed out" after being scaled up (O'Neill et al., 1986; Wu, 1999). To quantify ecological functions of complex urban ecosystems, therefore, their hierarchical structure needs to be treated explicitly.

### 4.3. Limitations and future development

At the current stage, HPM-UEM does not considers anthropogenic C emissions, which could account for more than 84% the total C emission in Phoenix (Koerner and Klopatek, 2002). Although biogenic C effluxes were detectable, especially during the daytime of growing season (Pataki et al., 2003, 2007), their overall magnitudes were relatively small compared to anthropogenic C emission in cities (Grimm et al., 2008b; Pataki et al., 2009). Similarly, a conservative estimation of urban C budget in the US, which did not include the fossil fuel C, indicated that the carbon stored in building is about three times the C stored in vegetation (Churkina et al., 2010). Therefore, a complete picture of urban C balance can only be gained by considering both ecological processes and anthropogenic material and energy fluxes (Pickett et al., 2001). Ecological modeling, such as exemplified by this study, can provide valuable information about spatial pattern and temporal dynamic of biogeochemical cycles in an urban ecosystem. When combined with inventory data of anthropogenic fluxes and pools (e.g., the VULCAN datasets developed by Gurney et al., 2009), the overall mass and energy balance of whole metropolitan region can be assessed.

Because during the model development we have prepared interfaces to link socioeconomic drivers to HPM-UEM at each ecosystem functional level (Fig. 1), the model can be further developed into a whole-urban-system model that integrates human and ecological dimensions (Churkina, 2008; Pataki et al., 2009). Socioeconomic dynamics can directly affect ecosystem functions by modifying the management regimes at the land-use scale (Martin et al., 2003) or indirectly influence biogeochemical processes by modifying landscape structure and inducing regional or local environmental (atmospheric and climate) changes (Idso, 2001; Arnfield, 2003). Statistical models (Martin et al., 2004; Jenerette et al., 2007), or agent-based simulations (Robinson et al., 2012) can be developed to quantify the effects of neighborhood socioeconomic statuses on the land-use management parameters in HPM-UEM simulations. Multiple-scaled land change models (e.g., the Spatial and Analytical Model Couplers (Moreira et al., 2009)), which integrate land change processes (driven by socioeconomic factors) at different hierarchical levels, can be directly coupled to HPM-UEM to guide patch dynamics at the regional to land-use scales (i.e., upgrading HPM-UEM from a patch mosaic to a patch dynamic model: HPD-UEM). At the same time, outputs from the HPM-UEM simulations, such as crop yields or the water consumption of vegetation, provide feedbacks to the economic module of the land change model systems (Moreira et al., 2009). While global climate models (GCM) driven by global greenhouse gas datasets could project the background environmental constraints (www.ipcc.ch), regional climate models (e.g., the WRF; Michalakes et al., 1998) and chemical transport models (e.g., CMAQ; Byun and Schere, 2006) driven by local air pollution and land management (e.g., irrigation) datasets could predict urban-induced environmental changes at the landscape level. At the same time, HPM-UEM and the coupled land change models can provide important land surface information (e.g., LAI, impervious surface area, and irrigated land area) as feedback to the regional climate models. A schematic representation of the multi-scale coupling mechanism between the HPM-UEM and land change models, climate models, and socioeconomic dynamics can be found in the Appendix, Fig. A1.

Currently, HPM-UEM does not address the spatial interactions between neighboring patches. Former studies indicated that horizontal C and N fluxes are driven by water flows across patch boundaries (Jenerette, 2004). Hydrological models like the SWAT (Santhi et al., 2006) can be coupled to HPM-UEM to assess the horizontal mass flow in the future. It should be noted that urban

hydrology is highly dynamic, controlled by the complex drainage system. A hydrological model describing the discharge processes in the sewer system as well as the surface processes (Thielen and Creutin, 1997) is necessary, where the drainage efficiency of land patches can be modeled as a function of its land type properties (e.g., a commercial center may have more efficient drainage system than a natural reserve), biogeophysical characteristics (e.g., slope), and the ecosystem functions (e.g., evapotranspiration rate).

The complex interactions between urban-induced climate change and global climate change make it difficult to predict future climate conditions in urbanized regions. In this study, climate change in Phoenix and its impacts on ecosystem functions were not further investigated. The sensitivity analysis (Fig. 3a) implied that future temperature rises due to global warming and UHI effects could have negative impacts on C storage in the Phoenix metropolitan region. However, it was also found that urban plant phenology could be altered in response to climate changes (Jochner et al., 2012). In high-latitude regions, the benefit from extended growth seasons may override the negative impacts of urban warming on ecosystem C sequestration. Future changes in precipitation could have important impacts on arid ecosystems in urbanized desert regions like Phoenix (Shen et al., 2005). Rapid expansions of oasis cities and agricultural lands have been found to cause precipitation increases from landscape to regional scales (Lioubimtseva and Cole, 2006). Although the over-irrigated urban vegetation may not be sensitive to precipitation change (Milesi et al., 2005), the remnant native deserts in the metropolitan regions could have more reactive and immediate response (Shen et al., 2009).

## 5. Conclusion

The complexity of human-dominated ecosystems, such as cities, stems from (1) spatiotemporal heterogeneity in the structure and function of human-altered landscapes, (2) the scale multiplicity of anthropogenic and environmental controls, (3) the diversity of biogeochemical processes and their nonlinear interactions, and (4) the intensive interaction between ecological processes and socioeconomic dynamics. Interdisciplinary urban research demands a new generation of ecological models that directly address the hierarchical structure of these systems in a spatially explicit manner. Our case study in the Phoenix metropolitan area has demonstrated that HPM-UEM is such a model that can help scale the local ecosystem functions to the urban landscape and regional levels, and improve our understanding of the complex interactions in human-dominated landscapes. The validity and generality of HPM-UEM, however, still need to be further tested in other urban landscapes of different regions. This is indeed our next step in the future development and application of HPM-UEM.

## Acknowledgements

The study was supported by the National Science Foundation of China under the grant #31170347 and #30970504, the National Science Foundation under grants #DEB-0423704 and BCS-1026865, Central Arizona-Phoenix Long-Term Ecological Research: CAP3: Urban Sustainability in the Dynamic Environment of Central Arizona. Portions of this work based on work supported by the National Science Foundation were completed while Nancy B. Grimm was working at the Foundation. Any opinions, findings, and conclusions expressed here are those of the authors and do not necessarily reflect the views of the Foundation. We thank the Ameriflux community for sharing the observational datasets. We are also grateful to Yun Ouyang, and Xiaoli Dong for their assistance with data preparation for this modeling project.

## Appendix A. Supplementary data

Supplementary data associated with this article can be found, in the online version, at http://dx.doi.org/10.1016/j.ecolmodel.2012.09.020.

## References

Alberti, M., 2010. Maintaining ecological integrity and sustaining ecosystem function in urban areas. Current Opinion in Environmental Sustainability 2 (3), 178–184, http://dx.doi.org/10.1016/j.cosust.2010.07.002.
Alig, R., Kline, J.D., Lichtenstein, M., 2004. Urbanization on the US landscape: looking ahead in the 21st century. Landscape and Urban Planning 69 (2–3), 219–234, http://dx.doi.org/10.1016/j.landurbplan.2003.07.004.
Arnfield, A.J., 2003. Two decades of urban climate research: a review of turbulence, exchanges of energy and water, and the urban heat island. International Journal of Climatology 23 (1), 1–26, http://dx.doi.org/10.1002/joc.859.
Baker, L.A., Hope, D., Xu, Y., Edmonds, J., Lauver, L., 2001. Nitrogen balance for the Central Arizona-Phoenix (CAP) ecosystem. Ecosystems 4, 582–602.
Barbour, M.G., 1973. Desert dogma reexamined: root/shoot productivity and plant spacing. American Midland Naturalist 89, 41–57.
Booch, G., 1994. Object-oriented analysis and design with applications, 2nd edition. Benjamin-Cummings Publishing Co., Inc, Redwood City, CA, USA.
Box, E.O., 1981. Macroclimate and Plant Forms: An Introduction to Predictive Modeling in Phytogeography. Dr. W. Junk, The Hague, 258 pp.
Brater, E.F., 1968. Steps toward a better understanding of urban runoff processes. Water Resource Research 4, 335–347.
Brazel, A.J., Johnson, M.D., 1980. Land-use effects on temperature and humidity in the Salt River valley, Arizona. Journal of the Arizona-Nevada Academy of Science 15, 54–61.
Buyantuyev, A., Wu, J., 2009. Urbanization alters spatiotemporal patterns of ecosystem primary production – a case study of the Phoenix metropolitan region, USA. Journal of Arid Environments 73, 512–520.
Buyantuyev, A., Wu, J., Gries, C., 2010. Multiscale analysis of the urbanization pattern of the Phoenix metropolitan landscape of USA: time, space and thematic resolution. Landscape and Urban Planning 94 (3–4), 206–217, http://dx.doi.org/10.1016/j.landurbplan.2009.10.005.
Byun, D., Schere, K.L., 2006. Review of the governing equations, computational algorithms, and other components of the models-3 community multiscale air quality (CMAQ) modeling system. Applied Mechanics Reviews 59, 51–77.
Cannell, M.G.R., Milne, R., Hargraeves, K.J., 1999. National inventories of terrestrial carbon sources and sinks: the U.K. experience. Climatic Change 42, 505–530.
Chen, G., Tian, H., Zhang, C., Liu, M., Ren, W., Zhu, W., Chappelka, A., Prior, S., Lockaby, G., 2012. Drought in the Southern United States over the 20th century: variability and its impacts on terrestrial ecosystem productivity and carbon storage. Climatic Change, http://dx.doi.org/10.1007/s10584-012-0410-z.
Churkina, G., 2008. Modeling the carbon cycle of urban systems. Ecological Modelling 216, 107–113.
Churkina, G., Brown, D.G., Keoleian, G., 2010. Carbon stored in human settlements: the conterminous United States. Global Change Biology 16 (1), 135–143, http://dx.doi.org/10.1111/j.1365-2486.2009.02002.x.
Ehlers, W., Hamblin, A.P., Tennant, D., Ploeg, R.R., 1991. Root system parameters determining water uptake of field crops. Irrigation Science 12, 115–124.
Farquhar, G.D., von Caemmerer, S., Berry, J.A., 1980. A biochemical model of photosynthetic $CO_2$ assimilation in leaves of C3 species. Planta 149, 78–90.
Gale, M.R., Grigal, D.F., 1987. Vertical root distributions of northern tree species in relation to successional status. Canadian Journal of Forest Research 17, 829–834.
George, K., Ziska, L.H., Bunce, J.A., Quebedeaux, B., Hom, J.L., Wolf, J., Teasdale, J.R., 2009. Macroclimate associated with urbanization increases the rate of secondary succession from fallow soil. Oecologia 159, 637–647.
Grimm, N.B., Faeth, S.H., Golubiewski, N.E., Redman, C.L., Wu, J., Bai, X., et al., 2008b. Global change and the ecology of cities. Science 319 (5864), 756–760, http://dx.doi.org/10.1126/science.1150195.
Grimm, N.B., Foster, D., Groffman, P., Grove, J.M., Hopkinson, C.S., Nadelhoffer, K.J., et al., 2008a. The changing landscape: ecosystem responses to urbanization and pollution across climatic and societal gradients. Frontiers in Ecology and the Environment 6 (5), 264–272, http://dx.doi.org/10.1890/070147.
Grimm, N.B., Redman, C., 2004. Approaches to the study of urban ecosystems: the case of Central Arizona-Phoenix. Urban Ecosystems 7, 199–213.
Groffman, P.M., Pouyat, R.V., Cadenasso, M.L., Zipperer, W.C., Szlavecz, K., Yesilonis, I.D., Band, L.E., Brush, G.S., 2006. Land-use context and natural soil controls on plant community composition and soil nitrogen and carbon dynamics in urban and rural forests. Forest Ecology and Management 236, 177–192.
Grossman-Clarke, S., Hope, D., Fernando, H., Stefanov, W., Zehnder, J., Hyde, P., 2005. Atmospheric Deposition $HNO_3$ Dry Deposition Fluxes in 1998 [Internet]. Arizona State University, CAP LTER, Metro Phoenix, AZ, Available from: http://caplter.asu.edu/data/?path=/exist/rest/db/datasets/util/xquery/getDatasetById.xql?_xsl=/db/datasets/util/xslt/datasetHTML.xsl&id=knb-lter-cap.264.1/
Gurney, K.R., Mendoza, D., Zhou, Y., Fischer, M., de la Rue du Can, S., Geethakumar, S., Miller, C., 2009. The Vulcan project: high resolution fossil fuel combustion $CO_2$ emissions fluxes for the United States. Environmental Science and Technology 43, http://dx.doi.org/10.1021/es900806c.
Haas, T.C., 1990. Kriging and automated variogram modeling within a moving window. Atmospheric Environment 24, 1759–1769.

Hall, S.J., Huber, D., Grimm, N.B., 2008. Soil $N_2O$ and NO emissions from an arid, urban ecosystem. Journal of Geophysical Research 113 (G1), 1–11, http://dx.doi.org/10.1029/2007JG000523.
Haxeltine, A., Prentice, I.C., 1996. BIOME3: An equilibrium terrestrial biosphere model based on ecophysiological constraints, resource availability, and competition among plant functional types. Global Biogeochemical. Cycles 10, 693–709.
Hope, D., Gries, C., Martin, C., 2005. Survey 200 – Trees (Dataset ID: 282_1). Central Arizona-Phoenix Long-Term Ecological Research online database, Available from http://caplter.asu.edu/data/?id=282 (updated 2005; cited 02.05.12).
Houghton, R.A., 2003. Revised estimates of the annual net flux of carbon to the atmosphere from changes in land-use and land management 1850–2000. Tellus B 55 (2), 378–390.
Houghton, R.A., Hobbie, J.E., Melillo, J.M., Moore, B., Peterson, B.J., Shaver, G.R., et al., 1983. Changes in the carbon content of terrestrial biota and soils between 1860 and 1980: a net release of $CO_2$ to the atmosphere. Ecological Monographs 53, 235–262.
Hutyra, L.R., Yoon, B., Alberti, M., 2011. Terrestrial carbon stocks across a gradient of urbanization: a study of the Seattle, WA region. Global Change Biology 17, 783–797.
Huxman, K.A., Smith, S.D., Neuman, D.S., 1999. Root hydraulic conductivity of *Larrea tridentata* and *Helianthus annuus* under elevated $CO_2$. Plant, Cell and Environment 22, 325–330.
Idso, C., 2001. An intensive two-week study of an urban $CO_2$ dome in Phoenix, Arizona, USA. Atmospheric Environment 35 (6), 995–1000, http://dx.doi.org/10.1016/S1352-2310(00)00412-X.
Imhoff, M.L., Bounoua, L., DeFries, R., Lawrence, W.T., Stutzer, D., Tucker, C.J., et al., 2004. The consequences of urban land transformation on net primary productivity in the United States. Remote Sensing of Environment 89 (4), 434–443, http://dx.doi.org/10.1016/j.rse.2003.10.015.
Jackson, R.B., Mooney, H.A., Schulze, E.D.A., 1997. Global budget for fine root biomass, surface area, and nutrient contents. Proceedings of the National Academy of Sciences of the United States of America 94, 7362–7366.
Jenerette, G.D., 2004. Landscape complexity and ecosystem processes of an urbanized arid region. ProQuest Dissertations and Theses. Arizona State University. 151 pp. Retrieved from http://search.proquest.com/docview/305218902?accountid=30505
Jenerette, G.D., Harlan, S.L., Brazel, A., Jones, N., Larsen, L., Stefanov, W.L., 2007. Regional relationships between surface temperature, vegetation, and human settlement in a rapidly urbanizing ecosystem. Landscape Ecology 22 (3), 353–365, http://dx.doi.org/10.1007/s10980-006-9032-z.
Jenerette, G.D., Wu, J., Grimm, N.B., Hope, D., 2006. Points, patches, and regions: scaling soil biogeochemical patterns in an urbanized arid ecosystem. Global Change Biology 12 (8), 1532–1544, http://dx.doi.org/10.1111/j.1365-2486.2006.01182.x.
Jochner, S.C., Sparks, T.H., Estrella, N., Menzel, A., 2012. The influence of altitude and urbanisation on trends and mean dates in phenology (1980–2009). International Journal of Biometeorology 56, 387–394.
Kaye, J.P., Majumdar, A., Gries, C., Buyantuyev, A., Grimm, N.B., Hope, D., et al., 2008. Hierarchical Bayesian scaling of soil properties across urban, agricultural, and desert ecosystems. Ecological Applications 18 (1), 132–145, PMID: 18372561.
Kaye, J.P., Mcculley, R.L., Burke, I.C., 2005. Carbon fluxes, nitrogen cycling, and soil microbial communities in adjacent urban, native and agricultural ecosystems. Global Change Biology 11, 575–587.
Koerner, B., Klopatek, J., 2002. Anthropogenic and natural $CO_2$ emission sources in an arid urban environment. Environmental Pollution 116 (Suppl.), S45–S51, PMID: 11833917.
Larcher, W., 1980. Physiological Plant Ecology. Springer-Verlag, New York, 303 pp.
Li, W., Ouyang, Z., Xiao, Y., 2011. Applying landscape ecological concepts in urban land-use classification. Acta Ecologica Sinica 31, 593–601 (in Chinese).
Lioubimtseva, E., Cole, R., 2006. Uncertainties of climate change in arid environments of central Asia. Reviews in Fisheries Science 14, 29–49.
Lohse, K.A., Hope, D., Sponseller, R.A., Allen, J.O., Grimm, N.B., 2008. Atmospheric deposition of nutrients across a desert city. Science of the Total Environment 402, 95–105.
Martin, C.A., Stabler, L.B., 2004. The relationship of homeowner practices and carbon acquisition potential of landscape plants to mesic and xeric designed Southwest residential landscapes. Acta Horticulturae 630, 137–141.
Martin, C.A., Warren, P.S., Kinzig, A.P., 2004. Neighborhood socioeconomic status is a useful predictor of perennial landscape vegetation in residential neighborhoods and embedded small parks of Phoenix, Arizona. Landscape and Urban Planning 69, 355–368.
Martin, C.A., Peterson, K.A., Stabler, L.B., 2003. Residential landscaping in Phoenix, Arizona, U.S.: practices and preferences relative to covenants, codes, and restrictions. Journal of Arboriculture 29, 9–17.
McDonald, R.I., 2008. Global urbanization: can ecologists identify a sustainable way forward? Frontiers in Ecology and the Environment 6 (2), 99–104, http://dx.doi.org/10.1890/070038.
McGuire, A.D., Sitch, S., Clein, J.S., Dargaville, R., Esser, G., Foley, J., et al., 2001. Carbon balance of the terrestrial biosphere in the twentieth century: analyses of $CO_2$, climate and land-use effects with four process-based ecosystem models. Global Biogeochemical Cycles 15, 183–206.
Mcpherson, E.G., 1998. Atmospheric carbon dioxide reduction by Sacramento's urban forest. Journal of Arboriculture 24 (4), 215–223.
Michalakes, J., Dudhia, J., Gill, D., Klemp, J., Skamarock, W., 1998. Design of a Next-Generation Regional Weather Research and Forecast Model: Towards Teracomputing. World Scientific, River Edge, NJ, pp. 117–124.
Milesi, C., Running, S.W., Dietz, J.B., Tuttle, B.T., 2005. Mapping and modeling the biogeochemical cycling of turf grasses in the United States. Environmental Management 36 (3), 426–438, http://dx.doi.org/10.1007/s00267-004-0316-2.
Miller, D.A., White, R.A., 1998. A conterminous united states multi-layer soil characteristics data set for regional climate and hydrology modeling. Earth Interactions 2, 1–25.
Miller, J.O., Galbraith, J.M., Daniels, W.L., 2004. Soil organic carbon content in frigid southern Appalachian Mountain soils. Soil Science Society of America Journal 68, 194–203.
Montaño, N.M., Jaramillo, V.J., García-Oliva, F., 2007. Dissolved organic carbon affects soil microbial activity and nitrogen dynamics in a Mexican tropical deciduous forest. Plant and Soil 295, 265–277.
Moreira, E., Costa, S., Aguiar, A., Câmara, G., Carneiro, T., 2009. Dynamical coupling of multiscale land change models. Landscape Ecology 24, 1183–1194.
Niemelä, J., 1999. Is there a need for a theory of urban ecology? Urban Ecosystems 3 (1), 57–65.
Nowak, D., 2006. Institutionalizing urban forestry as a "biotechnology" to improve environmental quality. Urban Forestry & Urban Greening 5 (2), 93–100, http://dx.doi.org/10.1016/j.ufug.2006.04.002.
Nowak, D.J., Crane, D.E., 2002. Carbon storage and sequestration by urban trees in the USA. Environmental Pollution 116 (3), 381–389, PMID: 11822716.
Nowak, D.J., Crane, D.E., 2000. The urban forest effects (UFORE) model: quantifying urban forest structure and functions. In: Hansen, M., Burk, T. (Eds.), Proceedings: Integrated Tools for Natural Resources Inventories in the 21st Century. IUFRO Conference. Boise, ID, August 16–20, 1998. U.S. Department of Agriculture, Forest Service, North Central Research Station, St. Paul, MN, pp. 714–720, General Technical Report NC-212.
Nowak, D.J., Stevens, J.C., Sisinni, S.M., Luley, C.J., 2002. Effects of urban tree management and species selection on atmospheric carbon dioxide. Journal of Arboriculture 28 (3), 113–122.
Oleson, K.W., Bonan, G.B., Feddema, J., Vertenstein, M., 2008. An urban parameterization for a global climate model. 2. Sensitivity to input parameters and the simulated urban heat island in offline simulations. Journal of Applied Meteorology and Climatology 47, 1061–1076.
O'Neill, R.V., DeAngelis, D.L., Waide, J.B., Allen, T.F.H., 1986. A Hierarchical Concept of Ecosystems. Princeton University Press, Princeton.
Parton, W.J., Stewart, J.W.B., Cole, C.V., 1988. Dynamics of C, N, P and S in grassland soils: a model. Biogeochemistry 5, 109–131.
Passioura, J.B., 1985. Roots and water economy of wheat. In: Day, W., Atkin, R.K. (Eds.), Wheat Growth and Modelling. Plenum Press, New York, p. 407.
Pataki, D.E., Alig, R.J., Fung, A.S., Golubiewski, N.E., Kennedy, C.A., Mcpherson, E.G., et al., 2006. Urban ecosystems and the North American carbon cycle. Global Change Biology 12 (11), 2092–2102, http://dx.doi.org/10.1111/j.1365-2486.2006.01242.x.
Pataki, D.E., Bowling, D.R., Ehleringer, J.R., 2003. Seasonal cycle of carbon dioxide and its isotopic composition in an urban atmosphere: anthropogenic and biogenic effects. Journal of Geophysical Research-Atmospheres 108 (D23), 4735, http://dx.doi.org/10.1029/2003JD003865.
Pataki, D.E., Xu, T., Luo, Y.Q., Ehleringer, J.R., 2007. Inferring biogenic and anthropogenic carbon dioxide sources across an urban to rural gradient. Oecologia 152 (2), 307–322.
Pataki, D.E., Emmi, P.C., Forster, C.B., Mills, J.I., Pardyjak, E.R., Peterson, T.R., et al., 2009. An integrated approach to improving fossil fuel emissions scenarios with urban ecosystem studies. Ecological Complexity 6 (1), 1–14.
Pataki, D.E., Carreiro, M.M., Cherrier, J., Grulke, N.E., Jennings, V., Pincetl, S., et al., 2011. Coupling biogeochemical cycles in urban environments: ecosystem services, green solutions, and misconceptions. Frontiers in Ecology and the Environment 9 (1), 27–36, http://dx.doi.org/10.1890/090220.
Pickett, S.T.A., Cadenasso, M.L., Grove, J.M., Nilon, C.H., Pouyat, R.V., Zipperer, W.C., Costanza, R., 2001. Urban ecological systems: linking terrestrial ecological, physical, and socioeconomic components of metropolitan areas. Annual Review of Ecology and Systematics 32, 127–157.
Pickett, S.T.A., Cadenasso, M.L., Grove, J.M., Boone, C.G., Groffman, P.M., Irwin, E., et al., 2011. Urban ecological systems: scientific foundations and a decade of progress. Journal of Environmental Management 92 (3), 331–362.
Pouyat, R.V., Carreiro, M.M., 2003. Controls on mass loss and nitrogen dynamics of oak leaf litter along an urban–rural land-use gradient. Oecologia 135, 288–298.
Pouyat, R.V., Yesilonis, I.D., Nowak, D.J., 2006. Carbon storage by urban soils in the United States. Journal of Environment Quality 35 (4), 1566–1575, http://dx.doi.org/10.2134/jeq2005.0215.
Pouyat, R.V., Pataki, D.E., Belt, K.T., Groffman, P.M., Hom, J., Band, L.E., 2007. Effects of urban land-use change on biogeochemical cycles. In: Canadell, J.G., Pataki, D.E., Pitelka, L.F. (Eds.), Terrestrial ecosystems in a changing world. Springer-Verlag, Berlin, pp. 45–58.
Prentice, I.C., Sykes, M.T., Cramer, W., 1993. A simulation model for the transient effects of climate change on forest landscapes. Ecological Modelling 65, 51–70.
Robinson, D.T., Shipeng, S., Hutchins, M., Riolo, R.L., Brown, D.G., Parker, D.C., Currie, W.S., Filatova, T., Kiger, S., 2012. Effects of land markets and land management on ecosystem function: a framework for modelling exurban land-changes. Environmental Modelling and Software, http://dx.doi.org/10.1016/j.envsoft.2012.06.016.
Running, S.W., Coughlan, J.C., 1988. A general model of forest ecosystem processes for regional applications, I. Hydrologic balance, canopy gas exchange and primary production processes. Ecological Modelling 42, 125–154.

Santhi, C., Srinivasan, R., Arnold, J.G., Williams, J.R., 2006. A modeling approach to evaluate the impacts of water quality management plans implemented in a watershed in Texas. Environmental Modelling & Software 21, 1141–1157.
Schaldach, R., Alcamo, J., 2007. Simulating the effects of urbanization, afforestation and cropland abandonment on a regional carbon balance: a case study for Central Germany. Regional Environmental Change 7, 137–148.
Schimel, J.P., Weintraub, M.N., 2003. The implications of exoenzyme activity on microbial C and N limitation in soil: a theoretical model. Soil Biology and Biochemistry 35, 549–563.
Schimel, D., Melillo, J., Tian, H., McGuire, A.D., Kicklighter, D., Kittel, T., et al., 2000. Contribution of increasing $CO_2$ and climate to carbon storage by ecosystems of the United States. Science 287, 2004–2006.
Sellers, P.J., 1985. Canopy reflectance, photosynthesis and transpiration. International Journal of Remote Sensing 6, 1335–1372.
Shen, W.J., Wu, J.G., Kemp, P.R., Reynolds, J.F., Grimm, N.B., 2005. Simulating the dynamics of primary productivity of a Sonoran ecosystem: model parameterization and validation. Ecological Modelling 189, 1–24.
Shen, W., Wu, J., Grimm, N.B., Hope, D., 2008. Effects of urbanization-induced environmental changes on ecosystem functioning in the Phoenix metropolitan region, USA. Ecosystems 11 (1), 138–155, http://dx.doi.org/10.1007/s10021-007-9085-0.
Shen, W., Reynolds, J.F., Hui, D., 2009. Responses of dryland soil respiration and soil carbon pool size to abrupt vs. gradual and individual vs. combined changes in soil temperature, precipitation, and atmospheric [$CO_2$]: a simulation analysis. Global Change Biology 15, 2274–2294.
Simon, H.A., 1962. The architecture of complexity. Proceedings of the American Philosophical Society 106, 467–482.
Sitch, S., Smith, B., Prentice, I.C., Arneth, A., Bondeau, A., Cramer, W., 2003. Evaluation of ecosystem dynamics, plant geography and terrestrial carbon cycling in the LPJ dynamic global vegetation model. Global Change Biology 9, 161–185.
Svirejeva-Hopkins, A., Schellnhuber, H.J., Pomaz, V.L., 2004. Urbanised territories as a specific component of the Global Carbon Cycle. Ecological Modelling 173 (2–3), 295–312, http://dx.doi.org/10.1016/j.ecolmodel.2003.09.022.
Thielen, J., Creutin, J.D., 1997. An urban hydrological model with high spatial resolution rainfall from a meteorological model. Journal of Hydrology 200, 58–83.
Trusilova, K., Churkina, G., 2008. The response of the terrestrial biosphere to urbanization: land cover conversion, climate, and urban pollution. Biogeosciences 5 (6), 1505–1515, http://dx.doi.org/10.5194/bg-5-1505-2008.
US Census Bureau [internet]. Available from: http://www.census.gov/popfinder/ [cited 2010].
Van der Ploeg, R.R., Beese, F., Strebel, O., Renger, M., 1978. The water balance of a sugar beet crop: a model and some experimental evidence. Zeitschrift für Pflanzenernährung und Bodenkunde 141, 313–328.
Veldkamp, A., Fresco, L., 1996. CLUE: a conceptual model to study the conversion of land use and its effects. Ecological Modelling 85, 253–270.
Vitousek, P.M., Mooney, H.A., Lubchenco, J., Melillo, J.M., 1997. Human domination of Earth's ecosystems. Science 277, 494–499.
Wang, H.F., Lopez-Pujol, J., Meyerson, L.A., Qiu, J.X., Wang, X.K., Ouyang, Z.Y., 2011. Biological invasions in rapidly urbanizing areas: a case study of Beijing, China. Biodiversity and Conservation 20, 2483–2509.
Wang, Y., Zhang, X., 2001. A dynamic modeling approach to simulating socioeconomic effects on landscape changes. Ecological Modelling 140, 141–162.
Wentz, E., Gober, P., Balling, R., Thomas, D., 2002. Spatial patterns and determinants of carbon dioxide in an urban environment. Annals of the Association of American Geographers 92, 15–28.
Wigmosta, M.S., Vail, L.W., Lettenmaier, D.P., 1994. A distributed hydrology-vegetation model for complex terrain. Water Resources Research 30 (6), 1665–1680.
Wu, J., 1999. Hierarchy and scaling: extrapolating information along a scaling ladder. Canadian Journal of Remote Sensing 25 (4), 367–380.
Wu, J., David, J.L., 2002. A spatially explicit hierarchical approach to modeling complex ecological systems: theory and applications. Ecological Modelling 153, 7–26.
Wu, J., Jenerette, G.D., David, J.L., 2003. Linking land-use change with ecosystem processes: a hierarchical patch dynamic model. In: Guhathakurta, S. (Ed.), Integrated Land-Use and Environmental Models. Springer, Berlin/Heidelberg/New York, pp. 99–119.
Yang, R., Friedl, M.A., Ni, W., 2001. Parameterization of shortwave radiation fluxes for nonuniform vegetation canopies in land surface models. Journal of Geophysical Research 106, 14275–14286.
Young, R.F., 2010. Managing municipal green space for ecosystem services. Urban Forestry & Urban Greening 9, 313–321.
Zeide, B., 1993. Primary unit of the tree crown. Ecology 74, 1598–1602.
Zhang, C., Tian, H.Q., Chen, G.S., Chappelka, A., Xu, X.F., Ren, W., Hui, D.F., Liu, M.L., Lu, C.Q., Pan, S.F., Lockaby, G., 2012. Impacts of urbanization on carbon balance in terrestrial ecosystems of the Southern United States. Environmental Pollution 164, 89–101.
Zhao, M., Kong, Z.H., Escobedo, F.J., Gao, J., 2010. Impacts of urban forests on offsetting carbon emissions from industrial energy use in Hangzhou, China. Journal of Environment Management 91 (4), 807–813, http://dx.doi.org/10.1016/j.jenvman.2009.10.010.
Ziska, L.H., Bunce, J.A., Goins, E.W., 2004. Characterization of an urban–rural $CO_2$/temperature gradient and associated changes in initial plant productivity during secondary succession. Oecologia 139, 454–458.